Ocean Engineering 340 (2025) 122314

Contents lists available at ScienceDirect

Ocean Engineering

journal homepage: www.elsevier.com/locate/oceaneng

Research paper

Multi-step ahead significant wave height forecasting using global and local view graph representation based on GRU model

Mohammed Diykh [a,b], Mumtaz Ali [a,*], Mehdi Jamei [b], Ramendra Prasad [c], Abdulhaleem H. Labban [d], Shahab Abdulla [a], Niharika Singh [a], Aitazaz Ahsan Farooque [b,e]

[a] UniSQ College, University of Southern Queensland, QLD, Australia
[b] Canadian Centre for Climate Change and Adaptation, University of Prince Edward Island, St Peters Bay, PE, Canada
[c] Department of Science, School of Science and Technology, The University of Fiji, Saweni, Lautoka, Fiji
[d] Department of Meteorology, Faculty of Environmental Sciences, King Abdulaziz University, 21589, Jeddah, Saudi Arabia
[e] Faculty of Sustainable Design Engineering, University of Prince Edward Island, Charlottetown, PE, Canada

ARTICLE INFO

Keywords:
Graph
Deep learning
Significant wave height
Prediction
Wave energy

ABSTRACT

Significant wave heights (SWH) are important to be predicted accurately for clean wave energy production, and beach erosion risks. The existing models lack the ability to analyse the dynamic behaviour of oceanic drivers, as a result, they cannot predict SWH at different forecasting horizons. In this paper, an innovative modelling scheme (termed as GLG-DL) based on graph deep learning which integrated global and local graph features has been designed to predict SWH. The global and local graph leaners enable GLG-DL model to capture the global information, and the local trends from oceanic drivers. The extracted graph representations are then used into the gated recurrent unit (GRU) based encoder and decoder to predict multistep ahead SWH for Palm Beach, Gladstone, and Albatross Bay stations, Australia. The GLG-DL model was compared with Auto-regression model (ARM), Auto-regressive multilayer perceptron (AR-MLP), Recurrent neural network (RNN), RNN based attention mechanism (RNN-AM), RNN based Long Short-term Memory (RNN-LSM), Spatial-temporal attention mechanism (STAM), and improved recurrent neural networks (SNN) models. The results demonstrated that the GLG-DL attained higher performance to forecast multistep ahead SWH for all stations. The GLG-DL model is beneficial in the application and optimization of clean energy resource generations worldwide.

1. Introduction

Despite significant development of wind power and solar PV in the global electricity mix and the persistent efforts to curb emissions to retain the global temperature rise to below 2 °C, the global power sector emissions rose 1.3 % to hit an all-time high in 2022 (REN21, 2023). One such renewable energy source, wave energy has the potential to narrow the emissions gap as it has higher energy density in comparison to wind and solar energy. Many countries are renewing their efforts to increase policy, research, and development for wave power. The wave energy sector is advancing significantly with various devices either in fabrication or preparing for deployment (OES, 2023). Supporting policy frameworks such as Australia's policy framework called the National Offshore Electricity Infrastructure Act-2021 offers a licensing scheme to enable the construction, operation and decommissioning of offshore renewable energy and offshore electricity infrastructure projects (Commonwealth of Australia, 2023). However, unlike solar energy, the wave energy does not have a clear day-night pattern, and this variable nature is one of the key limitations in wave energy generations.

Harmonization and interoperability is necessary for increased incorporation of wave energy and other variable energy into the grid for power generations and to overcome the minute scale intermittency, a faster response to demand changes needs essential digitization and automation (IRENA, 2022). To have dynamic and quick responsive wave energy power generation and demand response system to be used with conventional synchronous generation technologies, short-term significant wave height prediction is imperative. Effective prediction techniques for variables like significant wave height allow for adequate understanding of the distribution pattern, in facilitating synchronous wave energy integration. Ocean waves are highly irregular, unsteady with inconstant wave heights and lengths establishing inconsistent non-uniform data series (Raza Ul Mustafa et al., 2018). Other factors

* Corresponding author.
E-mail address: mumtaz.ali@unisq.edu.au (M. Ali).

https://doi.org/10.1016/j.oceaneng.2025.122314
Received 18 May 2025; Received in revised form 9 July 2025; Accepted 26 July 2025
Available online 1 August 2025
0029-8018/Crown Copyright © 2025 Published by Elsevier Ltd. This is an open access article under the CC BY license (http://creativecommons.org/licenses/by/4.0/).

that compounding the complexity of wave predictions are physical interactions such as refraction, diffraction, reflection, shoaling and trapping, bottom friction (Makarynskyy et al., 2002; Gorrell et al., 2011). In addition, the coastal effect and effects of complex bathymetry, propels a channelling effect creating additional constraint for physics-based models (Ibarra-Berastegi et al., 2016) while the machine learning artificial intelligence based models are data-dependent and does not get excessively affected by such local factors.

Scholars have relentlessly been designing and developing accurate and operational wave energy models. A time series modelling approach via auto-regressive-moving average (ARMA) model was used by Özger (2010), while Reikard, Robertson et al. (2015) in forecasting hourly power load used autoregressive integrated moving average (ARIMA). With time-varying parameters as inputs, the ARIMA model was accurate over short forecast horizons (Reikard et al., 2015). In addition, the random forest (RF) model was developed by Ibarra-Berastegi et al. (2016) to forecast wave energy at 3 and 16 h ahead forecast horizons in Portugal. The study found that the RF models outperformed the physics-based modelling approaches. It is well established that an artificial neural networks (ANN) model possesses good generalization capability that enables it to capture the nonlinear relationships between predictors and the objective variable, which has made is one of the most widely used ML techniques. Some notable examples of ANN models in ocean wave forecasting outside of the present study region includes: (Mérigaud et al., 2017); Australia (Adelaide, Tasmania, Sydney and Perth) (Burramukku, 2020); off the west coast of US (Özger, 2010) showed that these nonlinear ANN forecasting models worked well in capturing nonlinear sea states. Other modelling approaches such as Non-linear Autoregressive with exogenous input (NARX) (Gopinath and Dwarakish, 2015); adaptive-neuro-fuzzy-inference system (ANFIS) (Malekmohamadi et al., 2011); support vector machine (SVM) (Malekmohamadi et al., 2011); regressive-SVM (Mahjoobi and Adeli Mosabbeb, 2009); ensemble-extreme learning machine (ELM) (Kumar et al., 2018); grouping genetic algorithm-ELM (Cornejo-Bueno et al., 2016); hybrid-ELM (Ali and Prasad, 2019); C5 Tree-based forecasting model (Mahjoobi and Etemad-Shahidi, 2008) and multiple linear regression (MLR) model optimized by covariance-Weighted Least Squares (CWLS) MLR-CWLS model (Ali et al., 2020) has been applied for significant wave height forecasting. With evolution of big data analytics, computational capacity and the demand for short-term precise point forecasting, advanced competitive multivariate models are necessary for automation and quick demand response.

To improve the predictive accuracy of SWH, decomposition techniques such as Wavelet Transform WT, Empirical Model Decomposition (EMD) have been adopted in recent studies for example, Altunkaynak et al. (2024) designed a hybrid approach integrating WT, maximum overlap wavelet, and a fuzzy model. Their proposed model was tested using data collected from three stations located in the Atlantic Ocean. Chen et al. (2025) predicted SWH using variational mode decomposition based on LSTM, and temporal convolutional network. In that study, different prediction intervals including 24-h, 36-h, 48-h and 60-h were considered to evaluate the proposed model. Altunkaynak et al. (2023) applied Fuzzy logic approach based Singular Spectrum Analysis (SSA). The results obtained from Fuzzy logic based SSA were compared with WT based fuzzy logic model, and fuzzy logic model. Domala and Kim, 2023 examined the ability of combining Hodrick Prescot filter (HPF) with EMD to predict SWH. A LSTM was employed as a predictor, and it was integrated into EMD-HPF model. Guo et al., (2025) adopted Ensemble Empirical Mode Decomposition (EEMD) to predict SWH. The times series data was passed through EEMD, and the outputs of EEMD were sent into LSTM, SVR, and CNN.

The work of Zheng et al. (2023), Wang et al. (2024), Zhao et al. (2024) and other existing studies considered fixed relationships among oceanic time series data. However, the oceanic variables such as *MwH, ZCW, PEW, DRiC, SST, and SWH* impact each other dynamically non-linearly over the time. Therefore, it is required to develop a model which can reflect and capture the complex relationships among these variables. In this paper, we design a graph deep learning model (i.e., GLG-DL), considering both global and local features in graph representations. Each input variable was mapped as a node within the graph while the edges among nodes were constructed based on the statistical dependencies among the variables using correlation coefficient. This approach allows to capture the functional relationships and interactions among variables, and provide contextual learning compared to classical decomposition models. The global features depict the immediate dependencies among variables, while the local representations capture high-level long-term patterns. These graph representations are good for complex and noisy time series such as oceanic data. In addition, the global and local graph representations were combined using k-hop feature fusion which involves graph diffusion convolution on global graph, and linear weighed aggregation strategy *via* local graph.

In this study, local and global graph based deep learning model (GLG-DL) is designed that integrates local global graph features and local graph features to predict significant wave height. To represent the complex relationship among different variables of SWH time series data, complex network-based methods that employ graphs could be pivotal (Niepert et al., 2016; Sen et al., 2019; Rathore et al., 2021; Park et al., 2022; Sun et al., 2022; Tao et al., 2022). The key benefit is that GLG-DL model can combine deep learning methods with transformation techniques in predicting future values. In addition, in this GLG-DL model extracts the pertinent features using global graph learner and local graph learners, whereby the global graph leaner extracts the global information within the significant wave height time series, while the local graph learners capture to the local trends within the series. Successful application of graph-based DL models has been conducted in forecasting variables such as stock price (Tao et al., 2022), power systems (Sun et al., 2022), and wind speed (Rathore et al., 2021). The evaluation of their preciseness in forecasting significant wave height has not been studied with graph-based modelling and this study designs and evaluated the GLG-DL model.

2. Overview of the time series forecasting using graph domain approaches

Complex network-based methods employ graphs to represent the relationship among different variables of time series data (Niepert et al., 2016; Sen et al., 2019; Rathore et al., 2021; Park et al., 2022; Sun et al., 2022; Tao et al., 2022). Recently, several developed methods combined deep learning methods with transformation techniques to predict the future values of energy, electrical demand, stock price from time series data. The traditional deep learning model extract the local patterns; however, they can only be employed for the standard grid time series. Graph based deep learning generalized the traditional deep learning models to analyse the data of complex structures. Graph deep learning are usually employed the spectral or spatial domains (Liang et al., 2018; Zhang et al., 2019). In spatial domain, graph deep learning approaches are utilised Euclidean data of (time series) to form graphs to predict future values while the spectral domain is based on eigenvectors and eigenvalues to find the relationship for prediction.

Graph based approaches for time series prediction use adjacency matrix in spectral domain. Initially, the adjacency matrix is computed with a predefined threshold for training based on similarity among variables using Euclidean or Jaccard metric. However, calculating an adjacency matrix of graph requires prior knowledge which is not available for all-time series. In addition, static graphs are not suitable to reflect the dynamic characteristics of multivariate data. As a result, many methods based on graph have been designed to address this issue for example, Zhang, et al. (2019) designed graph model based on fixed Laplacian matrix during inference. Guo et al. (2019) combined adjacency and learned matrices to modify wight among nodes, however, a masked matrix was also employed as a Laplacian matrix. Graph structured learning, and adaptive graph-based models have also been

proposed to learn hidden graph structure from the data using adjacency and laten graph to extract features. However, the use of adaptively learned adjacency matrices cannot reflect the dynamic relationships of the time series. To tackle this problem, model based on adjacency matrices in a recurrent manner has been suggested in (Li et al., 2017; Guo et al., 2019; Sen et al., 2019) to design a model that captures the hidden characteristics of oceanic time series by integrating global and local graph learning models.

Physically, oceanic systems produce complex, and nonlinear behaviours that change over time. Traditional approaches often fail to extract the complex interdependencies among multivariate time series variables, as these models consider the static and non-Euclidean relationship, limiting their capability to extract dynamic interactions of oceanic parameters. For instance, changes in SST could affect wave height several hours later. The proposed model transferred the multivariate time series into a graph, where node is represented by one variable, and edges represent their functional dependencies. The core innovation of the proposed GLG-DL model lies by integration of global and local graph representations *via* GRU to improve the prediction of SWH. The global representations capture the shared trends and slow changing while the locals are employed to extract short-term dependencies and local fluctuations. The proposed model overcomes the limitations to handle nonlinear interactions and extract shared global trends. This leads to a better generalisation across different oceanic stations and improves prediction accuracy compared to traditional models.

3. Data description

3.1. Study locations

Australia is the world's largest island-continent, with a massive and diverse coastline. According to State of environment report 2021, about 87 % of Australia's population resides within 50 km of these shores. This possesses significant potential for the country to derive wave energy from coastal waves. This paper specifically focuses on three carefully chosen coastal stations in Queensland, Australia, i.e., Gladstone, Albatross Bay, and Palm Beach. These stations represent the varied geophysical and underwater (bathymetric) conditions across Australia's coast. Data at each site is collected using anchored oceanographic buoys specifically designed to measure wave characteristics. The timeframe considered is five years from 1 January 2018 to 31 December 2022. The station located in Gladstone, the monitoring instrument is Waverider Buoy Datawell 0.7m and the water depth of 16 m. The highest wave recorded here was of 4.39 m in May 2018 at 6am. The second station Albatross Bay is situated on the eastern shores of the Gulf of Carpentaria, Queensland recorded the highest wave of 6.603 m in March 2018 at 3pm. The water depth of 10 m at this site with AXYS TRIAXYS Directional Wave and current buoy as the monitoring instrument. The Palm Beach station located in Gold Coast; Queensland has Datawell MK4 Directional Waverider Buoy and the water depth of 23 m, recorded the highest wave of 10.131 m in December 2020 at 7:30am. A map depicting these coastal stations is provided in Fig. 1.

Although the water depths at the three stations are relatively close in magnitude, the bathymetric and geophysical settings are different in several important factors. For example, Palm Beach is placed on an open coast, and it is exposed to long-fetch wave energy from the South Pacific Ocean, with a relatively sandy seabed and steep continental shelf. While Gladstone station is positioned within a sheltered bay affected by industrial port activities, tidal estuarine dynamics, and muddy seabed conditions. However, Albatross Bay station is in a tropical, semi-enclosed coastal region with irregular bathymetry, including river inflows, and shallow bars which can pointedly chang energy dissipation. Despite these stations have similar depth range, the environmental differences produce diverse meteorological forcing, wave patterns, and spectral shapes at each station. These differences in wave behaviour across the three stations favours to validate the proposed GLG-DL model under different geophysical conditions.

3.2. Data collection and preparation

Coastal waves are characterised by the interaction with the coastline,

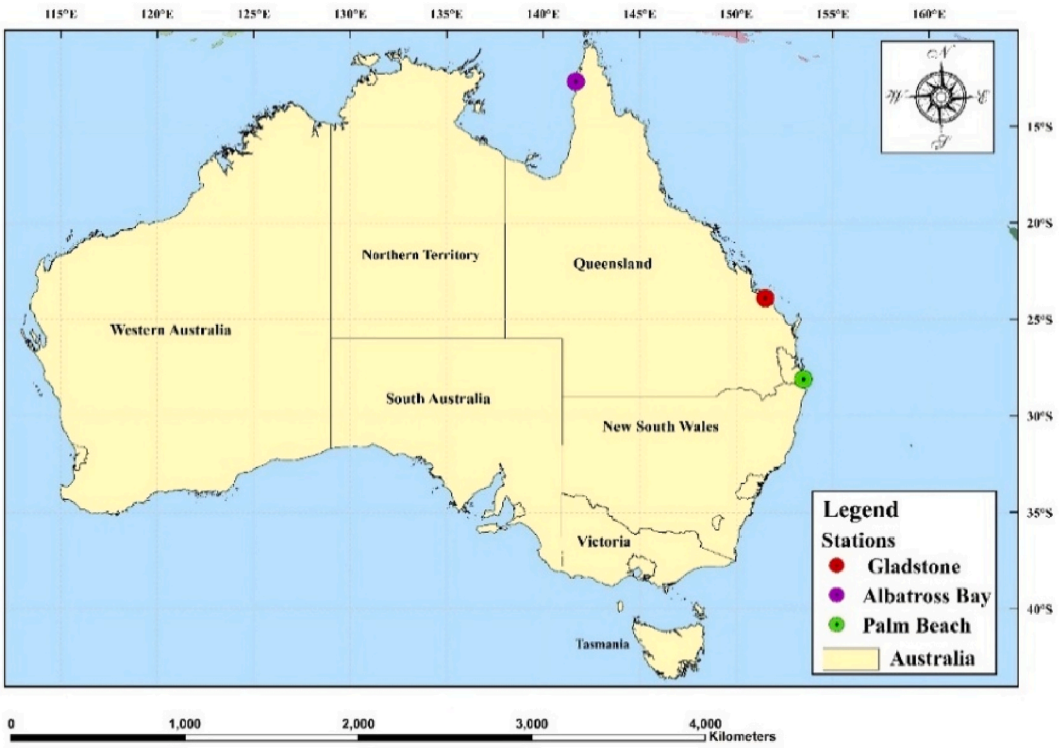

Fig. 1. Map of the coastal stations.

exhibit several key aspects of their nature. Their periodic nature arises from wind blowing over long stretches of open water, transferring energy to water surface, creating waves. These waves consist of crests (highest points) and troughs (lowest points) that alternates as the wave propagates. The data consist of the input variables which are recorded at a 30-min time interval. SWH is an average of the highest one-third of the waves in a record. This provides a more realistic picture of the typical wave size experienced visually. It is a more representative measure of the overall wave conditions and relates to the total wave energy available at the specific position. The energy carried by the ocean waves is proportional to the square of the wave height. SWH is one of the important predictor variables and has the largest statistical relationship with the objective variable. The maximum height (MwH) is the single tallest wave encountered in the recording period. Zero Up-Crossing Wave Period (ZCW) is the average time between consecutive instances where the wave surface crosses the mean water level in an upward direction (going from trough to crest). (ZCW) is another predictor that provides insights to the wave and reasonably affects SWH.

Peak energy wave period (PEW) is the wave period associated with the most energetic wave within the entire wave spectrum at a specific location. Direction (DRiC) is the direction from which the wave with the most energy is coming at a specific location and has a reasonable influence on SWH. Sea surface temperature (SST) is the temperature of the water at the ocean's surface and is measured in degrees Celsius by the wave monitoring buoys. Table 1 presents a summary, and some descriptive analysis of the data used in this paper whereas Fig. 2 shows the correlation in terms of heatmap of each variable with SWH. Fig. 3 reports the obtained CC values demonstrated that the variable MwH showed a consistent result with all three stations.

4. Methodology

4.1. Problem formulation

The purpose of forecasting model is to predict the future values of time series using historical data. The past data of ocean time series is defined as X_{nXmXf} where n is the length of the data, m the number of variables, and f features of each variable. We assume that the input for the proposed model is $X_{nXmXf} = \{X_{nXmXf_1}, X_{nXmXf_2}, \ldots, X_{nXmXf_n}\}$ where the first column refers to the target value. We used several different variables such as MwH, ZCW, DRiC, SST, and PEW to predict the SWH for multistep ahead in three regions. The primary feature of input time series is represented by X_{nXmXf}. It can be represented as weighted graph $G(v,E,A)$, where v is a set of nodes represent the input data, E is a set of edges, and A is adjacency matrix. We considered undirected graph to represent the time series data. Fig. 4 depicts time series from three station are being transferred into graphs.

$$\text{Where } (A > 0, when\ (v_1, v_2) \in E, \text{otherwise } A = 0 \quad (1)$$

Given historical data X of n variable, each variable is considered a node in graph $G(v,E,A)$, the objective is to learn function f to predict the target SWH for multistep ahead using the following equation.

$$X_{target} = f(X, G(v, E, A)) \quad (2)$$

Predicting SWH is challenging because variables in ocean wave time series are chaotic and exhibit irregular patterns. So, developing a model that can capture the hidden pattern of complex time series is essential to obtain a high prediction accuracy. This model can process the oceanic data directly on using graph-based deep learning and it can effectively acquire the global and local features.

4.2. General model architecture

Fig. 5 depicts the proposed model local and global graph features based on deep learning (GLG-DL) for significant wave height prediction. First, the global graph structure learning module is employed to extract the global relationships among the graph nodes. Second, in the local graph structure learning module is adopted used to capture the local features of graph. Third, the Gated Recurrent Units module is used for feature fusion to integrate the global and local features embedded in the graphs. Finally, the final fused feature set is sent to a Gated Recurrent Units based encoder, predictor for one ahead significant wave height forecasting. Algorithms 1, and 2 demonstrate graph learners with local and global graph representation.

4.2.1. Graph learning with Global feature representation

In this stage, we aimed to extract the global features of graphs. The global similarity is calculated among oceanic time series. The model consists of sample component, link predictor, feature extractor. A shared convolution kernel is employed to extract the global features of graph (Yu et al., 2016; Yu et al., 2017; Huang et al., 2019). In this paper, the input ocean time series X_{nXmXf} is fed into two layers of graph convolution networks *CNN*2. A fully connected layers *FCL* is used to reduce the data dimensionality of features in the feature extractor. A feature vector v_i is

Table 1
Descriptive statistics and geographic coordinates of the stations.

	Statistical index	MwH	ZCW	PEW	DRiC	SST	SWH
Gladstone	Minimum	0.19	2.26	1.66	0.51	11.65	0.10
Latitude = 23.53° S, Longitude = 151.30° E	Maximum	4.39	10.45	17.96	359.62	30.35	2.32
	Range	4.20	8.18	16.30	359.11	18.70	2.21
	Mean	1.23	4.16	6.77	89.54	22.74	0.71
	Std. Deviation	0.55	0.72	2.55	65.54	4.04	0.32
	Skewness	0.82	0.82	0.72	3.22	−0.54	0.74
	Kurtosis	0.55	2.21	0.328	10.45	−0.24	0.17
Albatross Bay	Minimum	0.07	1.10	1.57	0.00	5.00	0.03
Latitude = 12.41° S, Longitude = 141.41° E	Maximum	6.60	8.73	29.87	358.00	34.00	4.31
	Range	6.53	7.63	28.30	358.00	29.00	4.27
	Mean	0.74	3.19	4.09	189.63	28.39	0.41
	Std. Deviation	0.54	0.96	1.98	78.93	1.95	0.33
	Skewness	2.83	1.01	0.95	−0.30	−0.14	3.04
	Kurtosis	12.31	1.22	0.77	−1.35	−1.01	14.18
Palm Beach	Minimum	0.40	2.40	2.56	0.00	17.82	0.23
Latitude = 28.05° S, Longitude = 153.29° E	Maximum	10.13	18.18	20.00	359.30	29.22	53.00
	Range	9.72	15.77	17.43	359.30	11.40	52.76
	Mean	1.80	5.93	8.52	79.15	22.90	2.54
	Std. Deviation	0.80	2.09	2.74	21.57	2.36	8.66
	Skewness	1.51	1.46	0.19	1.65	0.05	5.63
	Kurtosis	4.05	2.40	−0.61	22.99	−1.28	29.88

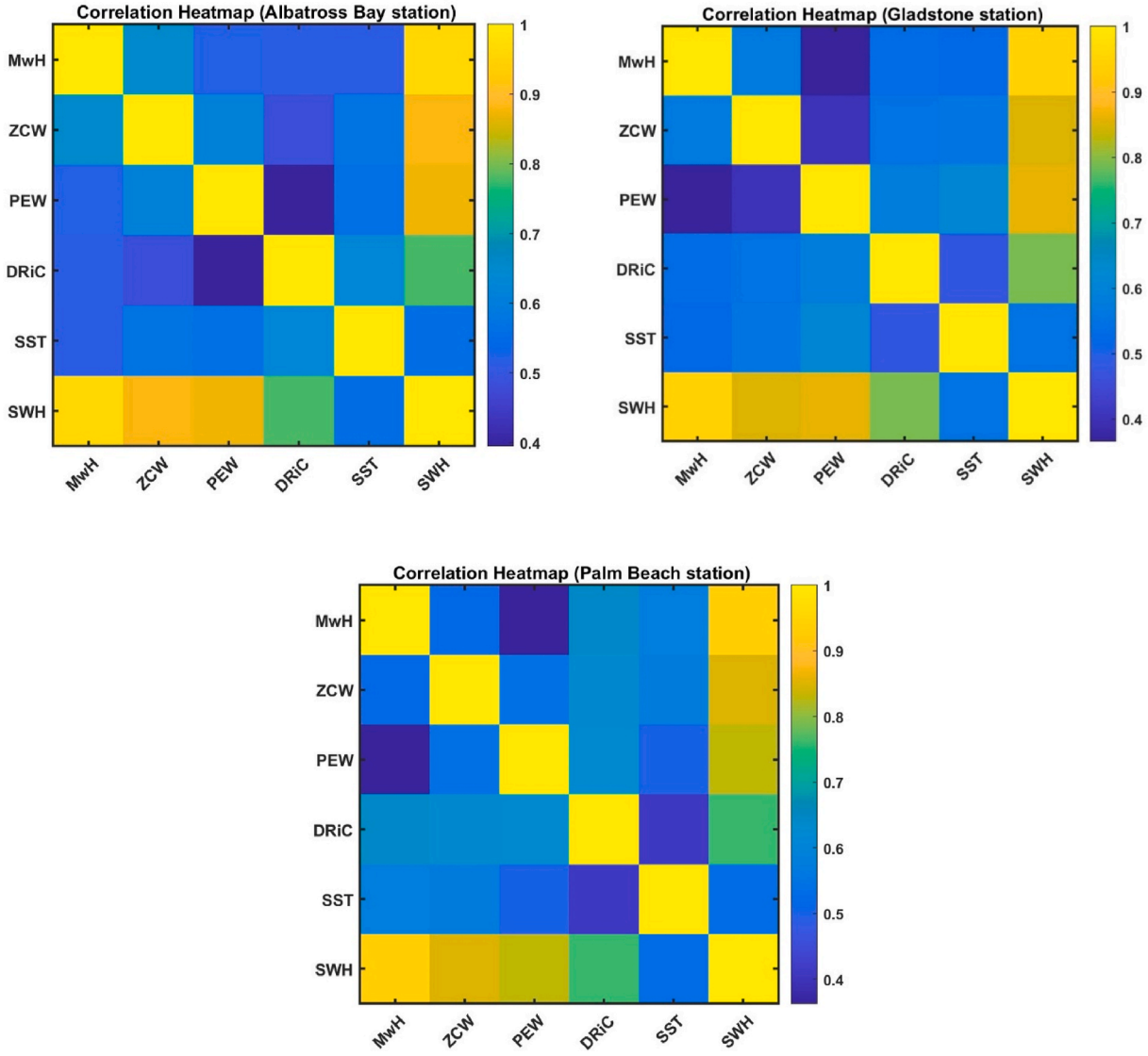

Fig. 2. Correlation Heatmap of each variable and significant wave height (SWH).

generated to denote the characteristics of *ith* node and is calculated from the following equation.

$$v_i = FCL\left(CNN2\left(X_{nXmXf}\right)\right) \tag{3}$$

Then, we concatenated a couple of victors (v_i, v_j) and we used a fully connected layer to produce edge in the link predictor.

$$E_{I,J} = FCL\left(v_i, v_j\right) \tag{4}$$

To identify the parameters of adjacency matrix of global graph A^{GLO}, we employed Gumbel reparameterization trick model. The A^{GLO} is generated using the following equation:

$$A^{GLO} = sigmoid\left[\log E_{I,J} \Big/ \left(i - E_{I,J}\right)\right) + \left(G^1_{i,j} - G^2_{i,j}\right) \tag{5}$$

Where $G^1_{i,j}, and\ \ G^2_{i,j}$ are gumball for all i,j.

4.2.2. Graph learning with local feature representation (LFR)

In this phase, the local feature representation is extracted from each graph. At each time stamp, time series data X_{nXmXf} is used an input to the proposed model which involves a series of local graph learners. We aggregated the features of each node. As a result, a sequence of features $\left\{f^1, f^1, \ldots., f^m\right\}$ is generated as follows:

$$f^i = AVG\left(X^{(m-1)\beta+1:m\beta}\right) \in R^{NxF} \tag{6}$$

Where m is the total number of datapoint, β is the size of data, AVG refers to an average aggregator. According to the Eq. (5), we required data of one day ahead to predict the significant wave height. Then, we used feature f^i to perform graph convolution on predefined graph G^{pre}, and global graph G^{glob} as follows:

$$P^i = Gconn\left(f^i, G^{pre}\right) \tag{7}$$

$$G^i = Gconn\left(f^i, G^{glob}\right) \tag{8}$$

Where $Gconn$ is the graph convolution with learnable parameters. Based on the output of Eq. (7), the dynamic embedding Nod^m_i for each node is calculated using the element wise multiplication between G^{pre}, and G^{glob}.

$$Nod^m_i = \tanh\left(\delta_p\left(P^i \omega\ vec\right) + \delta_G\left(G^i \omega\ vec\right)\right) \tag{9}$$

where vec is the static node embedding, δ_p and δ_G are parameters to control the weights, ω refers to the wise multiplication. The adjacency

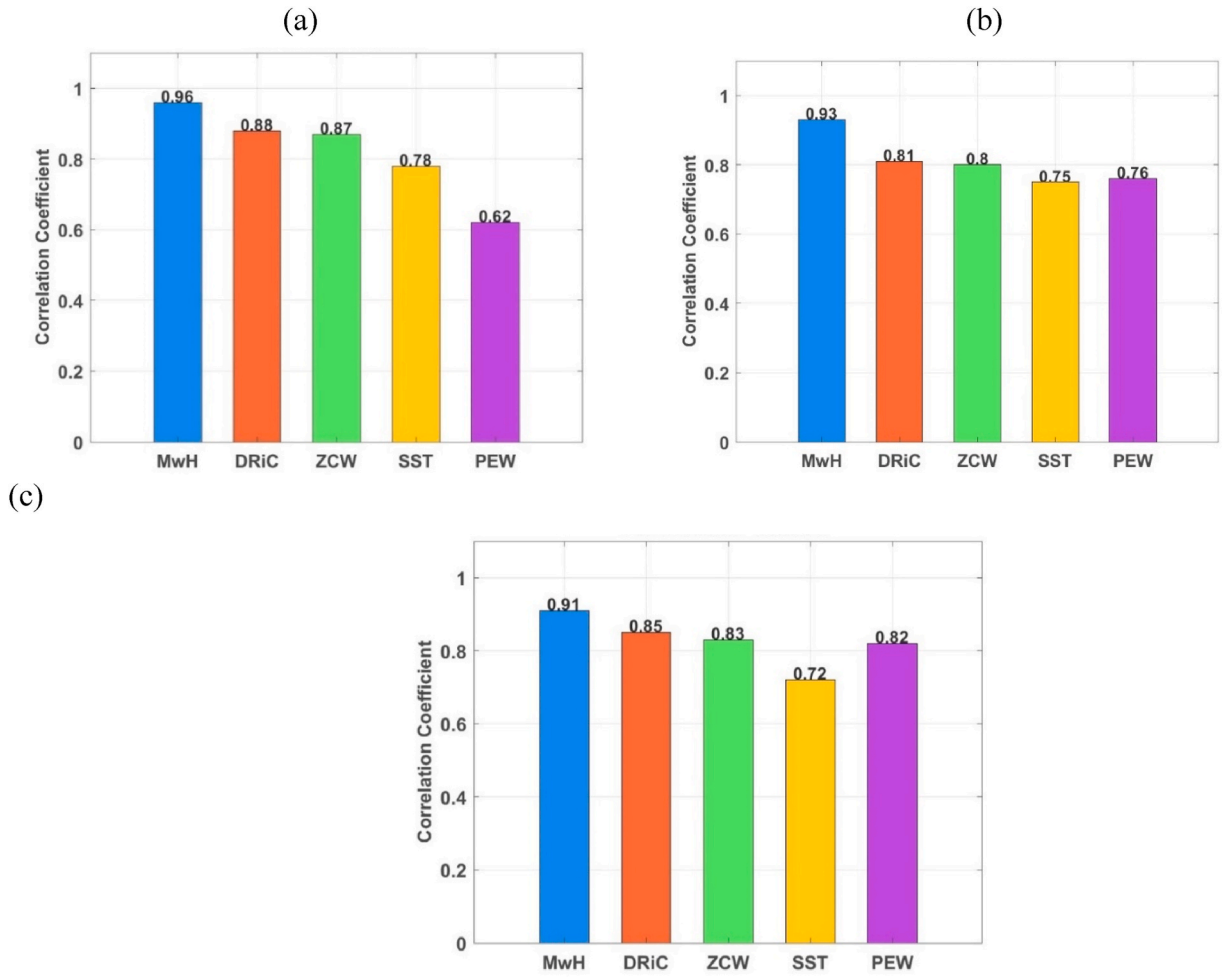

Fig. 3. Correlation coefficients of the proposed model based on different variables from (a) Albatross Bay, (b) Gladstone, and (c) Palm Beach stations.

matrix of local graph is computed using the similarity between pair variables. The element of adjacency matrix is calculated as follows:

$$A_{i,j}^{l_m} = RELU\left(\tau Nod_i^m, Nod_j^m\right) \tag{10}$$

Where τ is control parameters to adjust the capacity rate of activation function.

Algorithm 1. local feature representation

Input: node feature matrix, adjacency matrix, graph.

Output: graph local features $F = \left\{f^1, f^1, \ldots, f^m\right\}$

For each t→ T do

- $f^i = AVG\left(X^{(m-1)\beta+1:m\beta}\right)$
- $P^i = Gconn\left(f^i, G^{pre}\right)$
- $G^i = Gconn\left(f^i, G^{glob}\right)$
- $Nod_i^m = \tanh\left(\delta_p\left(P^i \omega\, vec\right) + \delta_G\left(G^i \omega\, vec\right)\right)$

End

$A_{i,j}^{l_m} = RELU\left(\tau Nod_i^m, Nod_j^m\right)$

Algorithm 2. Global feature representation

Input: Node feature matrix, temporal graph.

Output: Graph global representation $F = \left\{f^1, f^1, \ldots, f^m\right\}$

For each t→ T do

- $v_i = FCL\left(CNN2\left(X_{nXmXf}\right)\right)$
- $E_{I,J} = FCL\left(v_i, v_j\right)$

(*continued on next column*)

(*continued*)

- $A^{GLO} = sigmoid\left[\log E_{I,J}/(i - E_{I,J})\right) + \left(G_{i,j}^1 - G_{i,j}^2\right)$ (4)

End

4.2.3. Features integration based hierarchical learning model

We integrated the global and local graph features using k-hop feature fusion based on gated recurrent Unite. This phase involves three steps including graph diffusion convolution on global graph, and on local graph, and linear weighed aggregation. For global graph, bidirectional random graph walk is used to perform convolution graph. The bidirectional transition matrix which represents inflows and outflows graph walk, is calculated using diffusion convolution. Graph diffusion convolution on global graph is defined as

$$H^{(r-1)} * A^{glob} = \left[\omega_o + \omega_1\left(D_0^{-1}A^{glob}\right) + \omega_2\left(D_1^{-1}\left(A^{glob}\right)^t\right)\right]H^{(r-1)} \tag{11}$$

Where $H^{(r-1)}$ is the output of previous feature fusion layer, * denotes to the graph diffusion convolution, D_0, D_1 are in degree and out degree matrixes of A^{glob}, ω_1, ω_2 are hyperparameters of the model.

We defined the information propagation based on Eq. (11) above as

$$H^{(o)} = E^t \| H_{t-1} \tag{12}$$

$$H^{(k)} = \alpha\left(H^{(r-1)} * A^{glob}\right) + \beta\left(A^{lo}H^{(r-1)}\right) + \gamma\left(E^t \| H_{t-1}\right) \tag{13}$$

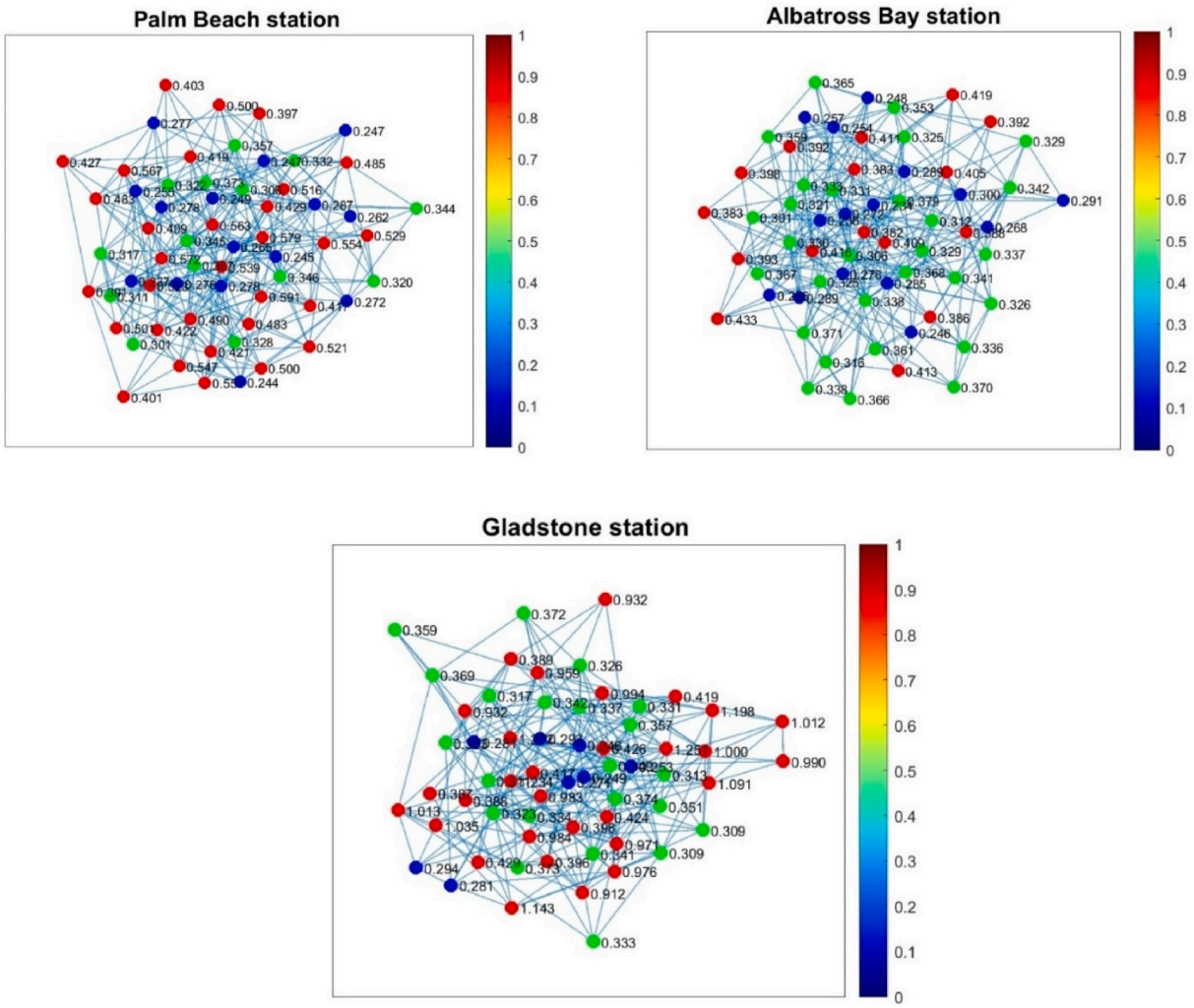

Fig. 4. A time series data from different stations are being mapped into an undirected graph.

Where * denotes to the multiplication, α, γ, β are hyperparameters that control the weights of model. To update gated recurrent unit, different integrated features representation is learned using the following equation.

$$\varnothing_p = \sum_{j=0}^{k} H^k \omega_p^i \tag{14}$$

Where p is the integrated feature representation which is used to update gate p, $\varnothing$ the selected information, ω_p^i is the leaner parameter, and k is depth of information propagation.

4.2.4. *Prediction model based on gated recurrent unit*

The gated recurrent Unit is updated using the following equation to integrate features repreparation.

$$H_t = N\varnothing H_{t-1} + (1-N)*C_t \tag{15}$$

$$C_t = \tanh\left(\varnothing\left[E^t \| (R_t \Phi H_{t-1})\right] + d_c\right) \tag{16}$$

The rest gate U_t and the updated gate are represented as

$$R_t = \xi(\phi_r, [E^t \| H_{t-1}] + d_r) \tag{17}$$

$$U_t = \xi(\phi_t, [E^t \| H_{t-1}] + d_u) \tag{18}$$

Where ϕ_r, ϕ_t are fusion feature layers, and ξ is activation function. The model passes through a sequence of encoder and decoder (prediction) to produce a prediction. The final hidden state of encoder to unitise the decoder. The decoder is trained by teacher forcing model using previous truth observation. During the testing, the prediction by the model is used for the prediction next observation.

5. Experimental results

We conducted extensive simulations to evaluate the proposed model for significant sea wave height prediction. We compared the proposed model with benchmarks and all results were recorded and discussed. The experiments were conducted on a personal computer powered with Windows 10 pro, Intel(R) core (TM) i7-7700HQ CPU @3 GHz and 8.00 GB memory. The MATLAB R2020b software was used to implement the proposed model.

5.1. *Evaluation metrics*

We employed several metrics to evaluate the proposed model. The evaluation metrics are chosen carefully, including relative square error (RSE), root mean square error (RMSE), empirical correlation coefficient (ECC), mean absolute error (MAE). With RMSE and RSE and MAE, lower values refer to high performance, Willmott's index agreement (WIA), correlation coefficient (CC), and high ECC values indicate that the proposed model perform very well (Che and Wang, 2010, Lafta et al., 2018; Abdulla et al., 2023).

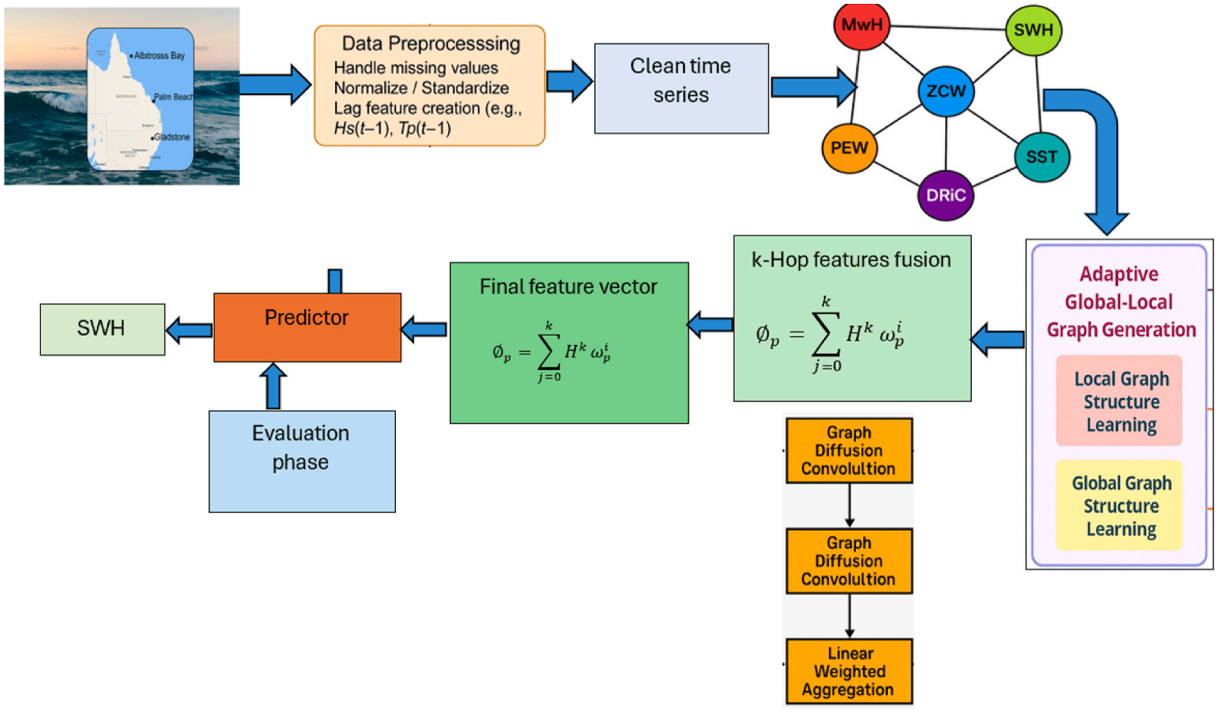

Fig. 5. Pipeline of the proposed model for multistep ahead significant wave height prediction.

$$RSE\ (\boldsymbol{x},\boldsymbol{y}) = \frac{\sqrt{(i,j) \in \varphi test\left(x_{i,j} - y_{i,j}\right)^2}}{\sqrt{(i,j) \in \varphi test\left(x_{i,j} - mean(x_i)\right)^2}} \tag{19}$$

$$ECC(x,y) = \frac{1}{n}\sum_{i=1}^{n} \frac{\sum_j \left(x_{i,j} - mean(x_i)\right)\left(y_{i,j} - mean(y_i)\right)}{\sqrt{\sum_{ij}\left(x_{i,j} - mean(x_i)\right)^2 \left(y_{i,j} - mean(y_i)\right)^2}} \tag{20}$$

$$RMSE = (x,y) = \sqrt{\frac{1}{n}\sum_{i=1}^{n}(x_i - y_i)} \tag{21}$$

$$MAE(x,y) = \frac{1}{n}\sum_{i=1}^{n}|x_i - y_i| \tag{22}$$

$$WIA = 1 - \frac{\sum_{i=1}^{n}(x_i - y_i)^2}{\sum_{i=1}^{n}\left(|x_i - \overline{x_i}| + |x_i - \overline{x_i}|\right)^2} \tag{23}$$

$$CC = \frac{\sum_{i=1}^{n}(x - \overline{x})(y - \overline{y})}{\sqrt{\sum_{i=1}^{n}(x - \overline{x})^2 \quad \sum_{i=1}^{n}(y - \overline{y})^2}} \tag{24}$$

Where x is the actual value, y is the predicted value, and $\overline{y}$ is the average value.

In addition, we employed Q-Q plot and regression to evaluate the proposed model. The quantiles of the actual values are plotted against the predicted values. According to the hypothesis of the Q-Q metric, a total of 30 % of the datapoints must lay below the reference value. However, the rest datapoints should be above the reference value. A line reference with A 45-degree is plotted. When the actual and predicted values have the same behaviours and distribution, all points are laid approximately along the reference line. With regression, the output value is between 0 and 1. The value 1 refers that the proposed model has a strong relationship with the truth ground model, and vice versa.

5.2. Training, evaluation strategy and parameters setting

To evaluate the proposed model, the mean absolute error (MAE) is calculated between the actual X_{nXmXf} and prediction results $X_{t:(t+s-1)}$. The base training loss is defined as

$$lose_{base}^{n}\left(\acute{X}_{n:(t+s-1)}, X_{t:(t+s-1)} + = \frac{1}{s}\sum_{n=1}^{t+s-1}\left|\acute{X}_{nXmXf}\right|\right| \tag{25}$$

The time series data is obtained from different cities in Queensland, Australia was used to evaluate the proposed model. the proposed model analysed the seasonality of significant sea wave height and trends, activities, as well as other parameters such as including MwH, ZCW, DRiC, SST and PEW to predict the significant wave height (SWH) for one day ahead. The pre-defined adjacency matrix is produced using a Gaussian threshold kernel to the Euclidean distance between any two points. A grid search was utilised to optimise with a batch size of 64. The learning rate of the proposed model was set to 0.1, 0.01, and 0.001. The dropout rate was set to 0.1, 0.2, and 0.3. We adopted a variable number of hidden units from (Rathore et al., 2021). since the dimension of the gated recurrent unit hidden state can significantly impact the accuracy of its forecasting. The values of the hyper-parameters ω_1, ω_2 were setup based on experimental results. The dataset was not randomly divided, but instead it was partitioned directly to preserve the temporal sequencing of the data. We used a 60 %, 20 %, 20 % split for training, validation, and testing, respectively, while maintaining the natural temporal order of time series. The model was trained on 60 %, then independently validated and testing on 20 % separately. This methodology was employed in this study to prevent data leakage and to protect temporal dependencies, which are vital for guaranteeing realistic and operationally evaluation in prediction tasks.

We investigated the influence of hyper-parameters on the performance of the proposed model. Each simulation was conducted 10 times, and we considered the MSE as a marker to identify the optimal parameters. First the model was configuring for Albatross Bay station, once the parameters were fixed, then the selected parameters of the proposed model were tested on Gladstone and Palm Beach stations. At each experiment, one parameter was tested, and the other were kept constant.

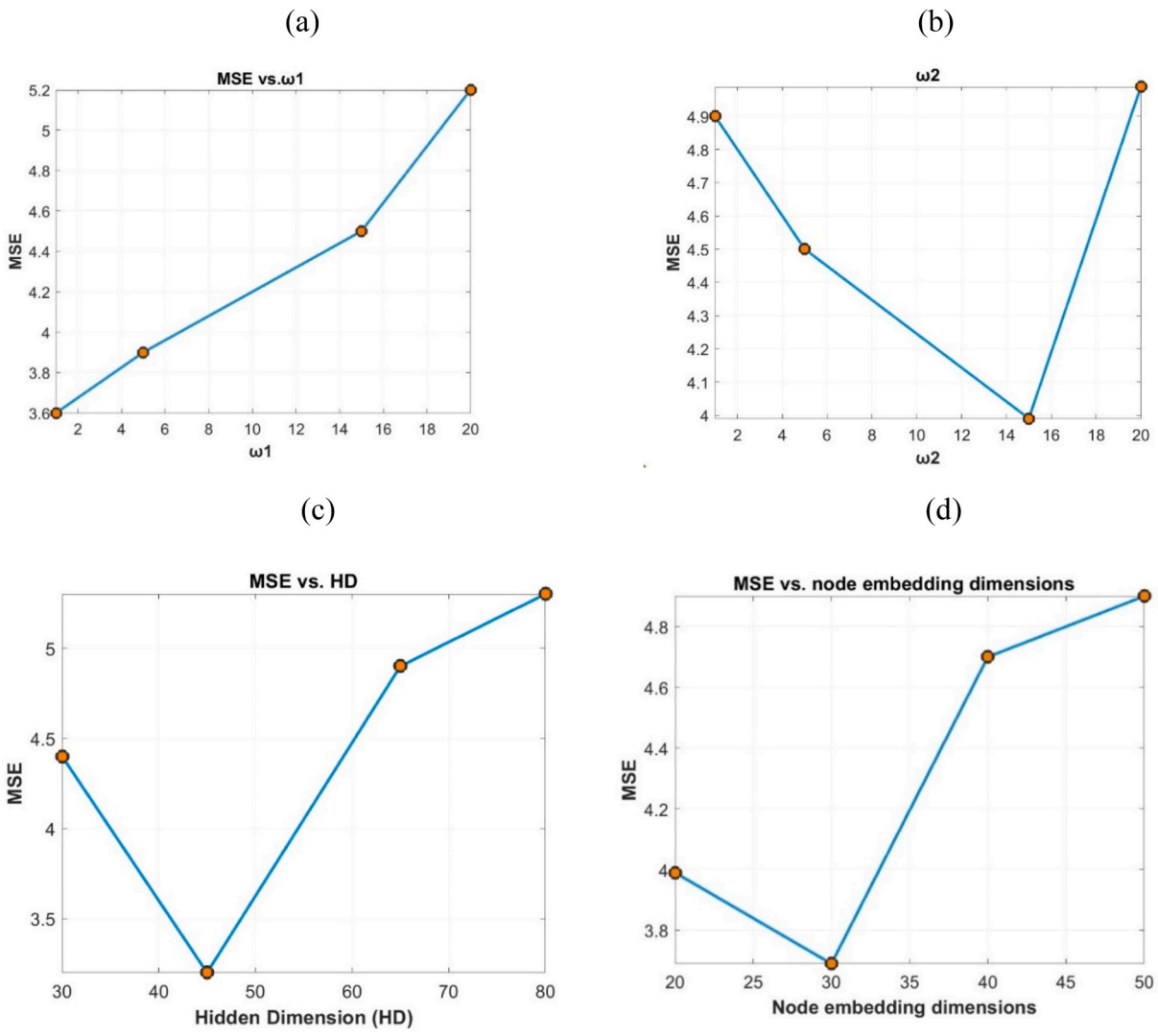

Fig. 6. Parameter's investigation of the proposed model GLG-DL (a), and (b) The effect of hyper parameter ω1 and ω2, (c) The node embedding dimension, and (d) The effect of hidden dimension.

Fig. 6(a–d) reports the results obtained of the hyper-parameters on the ocean dataset. The hyper-parameters $\omega 1$ and $\omega 2$ range were empirically chosen. From the obtained results, we found that decreasing $\omega 2$ and increasing $\omega 1$ improve the prediction accuracy.

The node embedding dimensions was set to 30 as shown in Fig. 6 (c). In addition, the hidden dimensions (HD)were set from 45 as shown in Fig. 6 (d). Fig. 6(a–d) showed that the performance proposed GLG-DP model was strengthened when the node embedding dimension was set to 30, and the hidden dimension was wet to 48. The proposed model GLG-DL parameters were fixed when the model recorded the lowest MAE.

5.3. Benchmarks

The proposed graph-based model was compared with several models to evaluate its performance against recent designed and standards model. Table 2 gives a brief summery about all baseline models used for the comparisons with the proposed graph-based model. The parameters of all models in Table 2 were selected carefully based on the simulation results.

Table 2
Baseline models for comparison with the proposed graph-based model.

	Model	Parameters	Abbreviation
1	Auto- regression based model (Che and Wang, 2010)	$\tau = 1$, $m = 3$	ARM
2	Auto-regressive based on multilayer perceptron (Zhao et al., 2020)	RBF kernel, $\lambda = 2^{-10}$	AR-MLP
3	Recurrent neural network model coupled with attention mechanism (Shih et al., 2019)	$Hu = \{25,75\}$, learning rate = 0.09.	RNN-AM
3	Recurrent neural networks based on fully connected Long Short-term Memory (Zhao et al., 2019)	One input gate, one forget gate, and one output gat	RNN-LSM
5	Recurrent neural networks (Smith and Jin, 2014)	population size set to 100	RNN
6	Spatial-temporal attention mechanism (Guo et al., 2019)	Chebyshev polynomial $K = 3$	STAM
7	Improved recurrent neural networks (Zhang et al., 2023)	Q = 0:01 and the number of Halton Points = 50	SNN

Where τ = *time scale*,m = *dimension*, λ = regression coefficient, Hu = number of hidden layers.

5.4. Main results

The results showed that the underlying properties of different ocean timeseries variables were easier to obtain through graph based deep learning model than other time series methods. The proposed graph based deep learning model was designed to predict to one-day ahead significant wave height (SWH) for three station Palm beach, Gladstone and Albatross stations in Queensland, Australia.

The all five variables including MwH, ZCW, DRiC, SST and PEW to predict the significant wave height (SWH) were tested to figure out the relation between these five variables and SWH. The SWH is nonstationary and irregular and inconsistent due to its nature. In this paper all five variables were sent to the proposed GLG-DL model to investigate the relationship and behaviour of each variable against SWH. Thorough simulations were conducted, at each experiment, one variable was removed and other sent to the proposed GLG-DL model. Our findings showed that not all variables have a strong relationship with SWH. For example, we found that the variable MwH was highly influenced the prediction results, and it showed a high correlation with SWH. In addition, we noticed that ZCW and DRiC had a good correlation with SWH. However, SST variable recorded the lowest correlation among all the variables.

5.4.1. The effect of fussing local and global graph features

Firstly, we examined the effects of using global and local graph features separately on the prediction rate and how the features fusion can improve the performance of the proposed model. Fig. 7 reports the prediction results in terms of MAE and correlation coefficient for three stations to investigate the effects of graph feature fusion. From the results, we can notice that the proposed model with global graph features achieved good prediction rates with all three stations, however, the performances was deteriorated dramatically with local graph features. By fusion the global and local graph characteristics, the prediction accuracy was noticeably increased. It can be noticed that the MAE and CC were improved over three stations after combining and fusing the global and local graph features. Form results in Fig. 7, its worthy to notice that the proposed GLG-DL model recorded high prediction rate with Albatross Bay station, while the lower results were scored with Palm Beach station over three experiments.

5.4.2. Performance comparisons with benchmarks

The proposed model was benchmarked with some well-known models from the literature. The oceanic time series was used as inputs to the proposed model as well as to the benchmarked models. Table 3 list the prediction results of the proposed GLG-DL model as well as ARM, AR-MLP, RNN-AM, RNN-LSM, RNN, STAM, and SNN for three stations named Albatross Bay, Palm Beach, and Gladstone stations. The comparisons were made in terms of relative square error (RSE), root mean square error (RMSE), empirical correlation coefficient (ECC), mean absolute error (MAE), and Willmott's index agreement (WIA). Table 3 reports the obtained results for Albatross Bay station. It can be notice that the proposed GLG-DL model recorded the highest prediction rate with RMSE = 2.310, MAE = 3.71, RSE = 0.164, ECC = 0.981, WIA = 0.98, CC = 0.99. However, the STAM model recorded the worst performance compared with other models. It recorded RMSE = 5.342, MAE = 7.89, RSE = 0.328, ECC = 0.652, WIA = 0.59, CC = 0.58. The RNN-LSM showed an acceptable performance and ranked the second highest prediction rate than ARM, AR-MLP, RNN-AM, RNN, STAM, and SNN

Table 3
Performance evaluation of the proposed model for Albatross Bay, Palm Beach, and Gladstone stations to predict SWH at the same time-step.

Model	RMSE	MAE	RSE	ECC	WIA	CC
Albatross Bay station						
ARM	3.186	5.95	0.365	0.840	0.80	0.80
AR-MLP	2.993	4.93	0.177	0.898	0.88	0.87
RNN-AM	3.928	4.91	0.182	0.891	0.77	0.76
RNN-LSM	2.894	4.87	0.157	0.854	0.85	0.88
RNN	5.964	6.94	0.391	0.704	0.62	0.61
STAM	5.342	7.89	0.328	0.652	0.59	0.58
SNN	6.216	6.94	0.289	0.676	0.64	0.65
Proposed GLG-DL	**2.310**	**3.71**	**0.164**	**0.981**	**0.98**	**0.99**
Palm Beach station						
ARM	3.7806	6.305	0.497	0.743	0.79	0.78
AR-MLP	3.001	5.103	0.207	0.808	0.84	0.83
RNN-AM	4.105	5.430	0.199	0.791	0.73	0.77
RNN-LSM	2.987	4.107	0.294	0.889	0.82	0.81
RNN	6.821	7.104	0.451	0.587	0.60	0.59
STAM	6.310	7.909	0.350	0.697	0.55	0.52
SNN	7.510	7.766	0.301	0.699	0.62	0.66
Proposed GLG-DL	**2.410**	**3.88**	**0.197**	**0.941**	**0.95**	**0.95**
Gladstone station						
ARM	3.513	6.10	0.398	0.874	0.82	0.82
AR-MLP	3.010	4.98	0.172	0.881	0.89	0.88
RNN-AM	4.100	4.97	0.192	0.773	0.78	0.71
RNN-LSM	3.175	4.80	0.199	0.801	0.86	0.87
RNN	6.543	7.21	0.421	0.604	0.59	0.63
STAM	6.102	7.90	0.395	0.627	0.61	0.60
SNN	6.979	7.12	0.299	0.631	0.62	0.62
Proposed GLG-DL	**2.677**	**3.73**	**0.164**	**0.961**	**0.96**	**0.97**

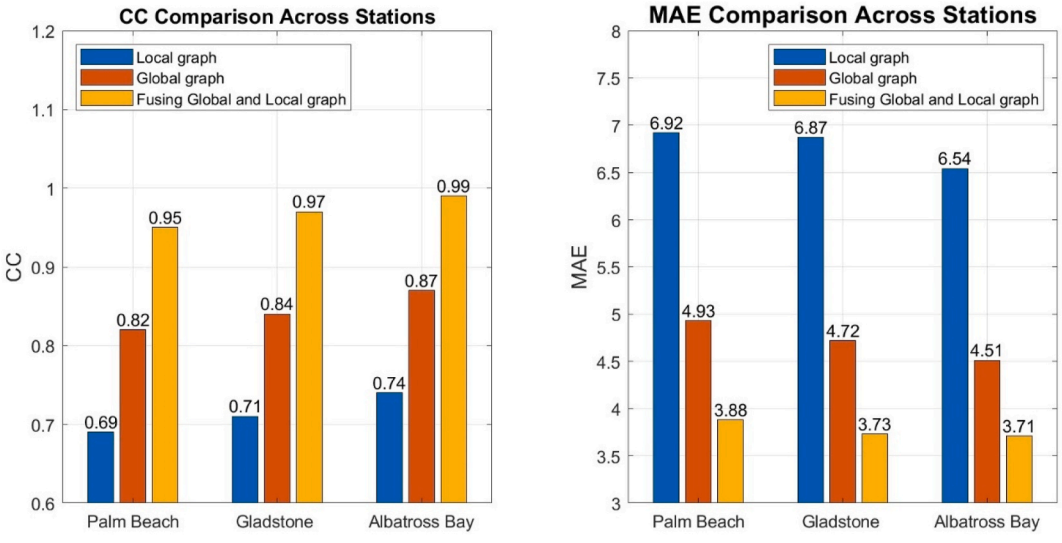

Fig. 7. Prediction results using local and global graphs features for all three stations.

models.

To investigate the performance of the proposed GLG-DL model for SWH prediction, A new experiment was conducted to explore for the benefit of fusing global and local graph features via GRU. The data from Palm beach was used in this experiment. Table 3 compares the performance all methods a long with the proposed model. The parameters of all models were empirically selected. We highlighted the best results in bold for all measures. For Palm Beach station in Table 3, we can notice that the performance of all models was slightly decreased. The mean reasons for that all models suffered from the irregularity behaviour of Palm station data. However, the GLG-DL model recorded the best prediction comparing to other models. It achieved RMSE = 2.410, MAE = 3.88, RSE = 0.197, ECC = 0.941, WIA = 0.95, CC = 0.95. The STAM model again recorded the worst performance compared with other models while the AR-MLP ranked the second highest precision rate.

In addition, SWH was also predicted for Gladstone station to examine the generalisation and validity of the proposed model and other previous models. Table 4 reports the results of all models using Gladstone station. The proposed GLG-DL was very promising because it obtained the best values of RMSE, MAE, RSE, ECC, WIA, and CC among all the state of art methods. Moreover, the proposed GLG-DL significantly outperformed all the alternatives method. It was worth mentioning that our graph based deep learning (i.e., proposed GLG-DL) model had the best performance over all stations and it was the ability to reveal all hidden features of oceanic data that exhibit non-stationary and unstable behaviour. We also can observe that the better performance from our proposed frameworks compared with all other models justify the reason behind establishing the more advanced framework that can deal with complex data such as oceanic data.

The proposed GLG-DL model along with other comparing models were evaluated on multistep ahead SWH forecasting. with different time intervals in Tables 4–6. The GLG-DL model achieved highest accuracy in terms of Albatross Bay station [RMSE = 2.032, MAE = 3.71, RSE = 0.164, ECC = 0.961, WIA = 0.98, CC = 0.99]; Palm Beach station [RMSE = 2.798, MAE = 3.77, RSE = 0.176, ECC = 0.954, WIA = 0.94, CC = 0.95]; Gladstone station [RMSE = 2.010, MAE = 3.01, RSE = 0.121, ECC = 0.969, WIA = 0.98, CC = 0.96] to forecast 30-min ahead SWH as compared to ARM, AR-MLP, RNN-AM, RNN-LSM, RNN, STAM, and SNN models (see; Table 4). Similarly, the proposed GLG-DL model outperformed against all comparing models to forecast 1-h (Table 5), and one-day (Table 6) ahead SWH prediction for Albatross Bay, Palm Beach, and Gladstone stations.

According to the results in Tables 4–6, the prediction accuracy was good for all timesteps, but the proposed GLG-DL attained highest precision at 30-mintes ahead, following by 1-h, and one-day ahead to predict SWH for these three stations. It is also noticed that RNN, SNN and RNN-AM improved in the short time interval (30-min) while lower prediction accuracy for one-day ahead. The proposed GDG-DL model achieved a stable and satisfactory performance over these different timesteps. The proposed GLG-DL model employed more effective graph of features to predict SWH by learning the global and local properties. This is because graph based deep learning model proved to be an efficient way to analyse time series that produce instable patterns and behaviour over different places and intervals.

The performance of the proposed **GLG-DL** model along with other benchmark comparing models were also assessed using the absolute forecasting error (FE). Fig. 8 report FE for all models in different stamp times. FE is one of the popular assessing metrics to examine how the prediction model is close to the actual SWH. Fig. 8 report the FE values (30-min, one day, 1 h ahead) of different models to predict SWH for Albatross Bay, Palm Beach and Gladstone stations. From Fig. 8, it can be observed that the proposed GLG-DL model acquired the lowest forecasting error FE for all three stations to predict SWH as compared to the benchmarking models. The best performance of the GLG-DL model was obtained in Albatross Bay, followed by Gladstone, and Palm Beach

Table 4
Performance evaluation of the proposed **GLG-DL** against comparing models to forecast 30-min ahead SWH for Albatross Bay, Palm Beach, and Gladstone stations.

Albatross Bay station						
Model	RMSE	MAE	RSE	ECC	WIA	CC
ARM	3.186	5.35	0.365	0.840	0.80	0.82
AR-MLP	2.993	3.93	0.177	0.898	0.88	0.88
RNN-AM	3.948	3.91	0.182	0.791	0.79	0.80
RNN-LSM	2.102	4.10	0.152	0.904	0.89	0.90
RNN	5.964	6.94	0.391	0.604	0.62	0.61
STAM	5.342	7.89	0.328	0.612	0.59	0.58
SNN	6.216	6.94	0.289	0.676	0.64	0.65
The proposed GLG-DL	**2.032**	**3.71**	**0.164**	**0.961**	**0.98**	**0.99**
Palm Beach station						
Model	RMSE	MAE	RSE	ECC	WIA	CC
ARM	3.204	5.28	0.301	0.892	0.80	0.81
AR-MLP	3.731	5.46	0.210	0.798	0.78	0.79
RNN-AM	4.001	5.91	0.201	0.799	0.71	0.77
RNN-LSM	2.210	4.11	0.291	0.820	0.84	0.84
RNN	5.312	6.76	0.367	0.621	0.59	0.60
STAM	6.21	6.54	0.313	0.651	0.66	0.63
SNN	6.290	6.99	0.299	0.620	0.64	0.65
The proposed GLG-DL	**2.798**	**3.77**	**0.176**	**0.954**	**0.94**	**0.95**
Gladstone station						
Model	RMSE	MAE	RSE	ECC	WIA	CC
ARM	3.754	5.54	0.254	0.838	0.81	0.83
AR-MLP	2.290	3.99	0.153	0.871	0.88	0.89
RNN-AM	2.991	3.97	0.198	0.884	0.79	0.80
RNN-LSM	2.791	4.10	0.159	0.851	0.89	0.89
RNN	4.931	6.01	0.323	0.621	0.64	0.64
STAM	4.989	6.85	0.302	0.622	0.59	0.66
SNN	5.32	5.93	0.311	0.792	0.69	0.70
The proposed GLG-DL	**2.010**	**3.01**	**0.121**	**0.969**	**0.98**	**0.96**

Table 5
Performance evaluation of the proposed **GLG-DL** against comparing models to forecast 1 h ahead SWH for Albatross Bay, Palm Beach, and Gladstone stations.

Albatross Bay station						
Model	RMSE	MAE	RSE	ECC	WIA	CC
ARM	3.101	5.01	0.231	0.829	0.83	0.83
AR-MLP	2.210	4.10	0.161	0.862	0.88	0.88
RNN-AM	3.103	4.02	0.192	0.785	0.78	0.79
RNN-LSM	2.897	4.91	0.160	0.866	0.86	0.86
RNN	5.321	6.16	0.382	0.652	0.62	0.62
STAM	5.132	6.98	0.342	0.520	0.57	0.58
SNN	6.121	6.43	0.273	0.602	0.65	0.67
The proposed GLG-DL	**2.021**	**3.21**	**0.132**	**0.953**	**0.96**	**0.95**
Palm Beach station						
Model	RMSE	MAE	RSE	ECC	WIA	CC
ARM	3.204	5.28	0.301	0.892	0.80	0.81
AR-MLP	3.731	5.46	0.210	0.798	0.78	0.79
RNN-AM	4.001	5.91	0.201	0.799	0.71	0.72
RNN-LSM	2.210	4.11	0.291	0.820	0.84	0.84
RNN	5.312	6.76	0.367	0.621	0.59	0.60
STAM	6.21	6.54	0.313	0.651	0.66	0.63
SNN	6.290	6.99	0.299	0.620	0.64	0.65
The proposed GLG-DL	**2.798**	**3.57**	**0.176**	**0.924**	**0.92**	**0.93**
Gladstone station						
Model	RMSE	MAE	RSE	ECC	WIA	CC
ARM	3.754	5.54	0.254	0.898	0.81	0.83
AR-MLP	2.290	3.99	0.153	0.871	0.88	0.89
RNN-AM	2.991	3.97	0.198	0.884	0.79	0.80
RNN-LSM	2.791	4.10	0.159	0.851	0.89	0.89
RNN	4.931	6.01	0.323	0.921	0.64	0.64
STAM	4.989	6.85	0.302	0.922	0.59	0.60
SNN	5.99	6.93	0.391	0.942	0.68	0.69
The proposed GLG-DL	**2.010**	**3.01**	**0.121**	**0.799**	**0.98**	**0.96**

Table 6
Performance evaluation of the proposed **GLG-DL** against comparing models to forecast one-day ahead SWH for Albatross Bay, Palm Beach, and Gladstone stations.

Albatross Bay station						
Model	RMSE	MAE	RSE	ECC	WIA	CC
ARM	3.210	5.98	0.371	0.789	0.76	0.77
AR-MLP	3.999	4.95	0.276	0.796	0.77	0.79
RNN-AM	3.980	4.96	0.287	0.704	0.69	0.70
RNN-LSM	3.897	4.91	0.260	0.806	0.80	0.80
RNN	5.970	6.96	0.399	0.607	0.54	0.57
STAM	5.452	7.2	0.401	0.572	0.50	0.52
SNN	6.298	6.949	0.394	0.586	0.53	0.57
The proposed GLG-DL	**3.01**	**4.21**	**0.2011**	**0.921**	**0.92**	**0.93**
Palm Beach station						
Model	RMSE	MAE	RSE	ECC	WIA	CC
ARM	3.751	6.18	0.392	0.710	0.73	0.75
AR-MLP	4.321	5.11	0.288	0.700	0.72	0.74
RNN-AM	4.760	5.02	0.312	0.680	0.65	0.69
RNN-LSM	3.985	4.99	0.299	0.770	0.78	0.76
RNN	6.440	7.06	0.421	0.517	0.51	0.52
STAM	5.9583	7.71	0.434	0.501	0.50	0.50
SNN	6.982	7.21	0.471	0.511	0.51	0.53
The proposed GLG-DL	**3.35**	**4.84**	**0.299**	**0.897**	**0.90**	**0.91**
Gladstone station						
Model	RMSE	MAE	RSE	ECC	WIA	CC
ARM	3.754	6.75	0.399	0.877	0.80	0.81
AR-MLP	3.211	4.99	0.180	0.890	0.87	0.87
RNN-AM	4.768	4.99	0.199	0.780	0.72	0.70
RNN-LSM	3.190	4.87	0.198	0.886	0.85	0.86
RNN	6.751	7.64	0.476	0.621	0.58	0.62
STAM	6.001	7.87	0.389	0.610	0.62	0.61
SNN	6.954	7.01	0.297	0.621	0.62	0.61
The proposed GLG-DL	**2.757**	**3.77**	**0.166**	**0.953**	**0.95**	**0.94**

stations. However, most of the benchmark comparing models showed a lower prediction performance with higher FE values.

Another metric was considered to assess the generalisation of the proposed model. In this experiment, Nash-Sutcliffe Efficiency (NSE) was adopted to test the performance of the proposed GLG-DL model. Fig. 9 illustrate the performances of the proposed GLG-DL model against the ARM, AR-MLP, RNN-AM, RNN-LSM, RNN, STAM, and SNN models in term of NSE with different time intervals. In this experiment, 30 min, I hour and one day time interval were considered to evaluate the proposed model. The results support our findings in Tables 4–6 Fig. 9 authenticate that the proposed GLG-DL model shows strong prediction accuracy for all three stations to forecast multistep (i.e., 30-min, 1-h, and one-day) ahead SWH. The results demonstrated that the comparing models showed low performance for 30 min ahead SWH prediction. However, the proposed GLG-DL model approved the ability of graphs in dealing with different intervals times.

The results in Fig. 10 confirms the superiority of the proposed GLG-DL over the benchmark comparing models based on Legates and McCabe's (LM). The results confirm that GLG-DL was effective tool to capture and analyse the complex pattern of oceanic data. The use of graph to model the oceanic data has shown that the mapping of oceanic data into graph improved the prediction accuracy of SWH by capturing the hidden patterns and features. Fig. 10, it can be noticed that all models showed a lower performance except GLG-DL when applied to predict multistep ahead SWH for all three stations.

5.4.3. Performance evaluation using regression plots

The regression plot was used to examine the behaviour of the proposed GLG-DL mode towards the observation in Fig. 11(a–c) for different time steps. From the results obtained, the proposed GLG-DL model shows a high relationship with the actual SWH for 30-min, 1-h, and one-day forecast horizon in Albatross Bay station. The proposed GLG-DL recorded a high forecasting rate R = 0.97 to predict SWH, compared with ARM, SNN, STAM, RNN, RNN-LSM, RNN-AM, AR-LMP and ARM. Although the AR-PML model recorded the second highest forecasting rate with R = 0.88, but it was lower than the proposed GLG-DL model (Fig. 11 (a)).

Fig. 11 (b) shows the regression plots of the proposed GLG-DL model against comparing counterpart models for 1 h prediction ahead. The results in Fig. 11 (b) demonstrates the ability of the proposed model in SWH prediction SWH. The GLG-DL did not show a high fluctuation compared to the results of Albatross station. It recorded a regression of R = 0.9770 which was the highest forecasting rate compared to ARM, SNN, STAM, RNN, RNN-LSM, RNN-AM, AR-LMP and ARM. The RNN-LSM showed a good agreement with the observation. The RNN-LSM recorded R = 0.883, while the SNN exhibited a negative agreement with the actual SWH, and the SNN scored the lowest R = 0.68.

The results for one day head forecasting were presented in Fig. 11 (c). The performance of the proposed GLG-DL again showed a high prediction rate, and it did not affect when it was tested with different stations and different time steps. It was noticed that our graph learning modules proved to be an effective tool in terms of improving oceanic data prediction. The combination of local and graph features increased the precision of model compared with the traditional and previous models ARM, SNN, STAM, RNN, RNN-LSM, RNN-AM, AR-LMP and ARM. The AR-MLP model recorded the second highest prediction rate with R = 0.878, however, the SNN ranked the worst model with performance with R = 0.67. From the results in Fig. 10, the only model that showed better prediction rate was the proposed GLG-DL model. The proposed model scored the highest R = 0.99, R = 0.97, R = 0.96 with Albatross Bay, Gladstone, and Palm Beach stations respectively.

5.4.4. Performance evaluation using Taylor diagram

In this experiment, Taylor diagrams was utilised to evaluate the proposed model accuracy. It's a graphical metric that summarizes how closely a set of models matches the actual SWH. The similarity between the proposed model and the truth base is measured in terms of correlation, root-mean-square difference, and standard deviations. It has been used widely to assess the behaviour of complex models. The centred root mean squares difference between the predicted and observed samples refers to the distance to the point on the x-axis that is identified as observed/actual/reference (ref). While ethe standard deviation indicates to the proportional to the radial distance from the origin. Fig. 12 (a, b, c) shows the Taylor diagram of the proposed GLG-DL model compared with other models for three stations. With Albatross Bay, and Gladstone stations, the proposed GLG-DL model shows a high agreement with the observation/ref SWH compared with other models. In addition, AR-MLP, and RNN-LSM exhibit a good correlation with the actual observation/red. However, RNN, and STAM showed a poor performance, and they were negatively correlated with the main observation.

The best performance of the proposed GLG-DL model was recorded with Albatross Bay station, followed with Gladstone, and Beach stations. Our finding showed that oceanic data exhibit a complex behaviour, using the traditional deep learning-based model cannot reflect the relationships and hidden patterns of this type of data. So, it requires more sophisticated approach to analyse the data to find the main attributes among the variables that are highly correlated with the observation.

6. Discussion

A novel graph based deep learning (i.e., GLG-DL) model has been designed which integrate global and local graph features to predict multistep ahead significant wave height (SWH). The oceanic time series input predictors are mapped as networks where the global graph learner and local graph learner are adopted to extract the features. The global graph leaner captures the global information across oceanic timeseries, and local graphs learner is used to extract the local trends. The extracted features are then passed into the unit-based encoder and decode i.e.,

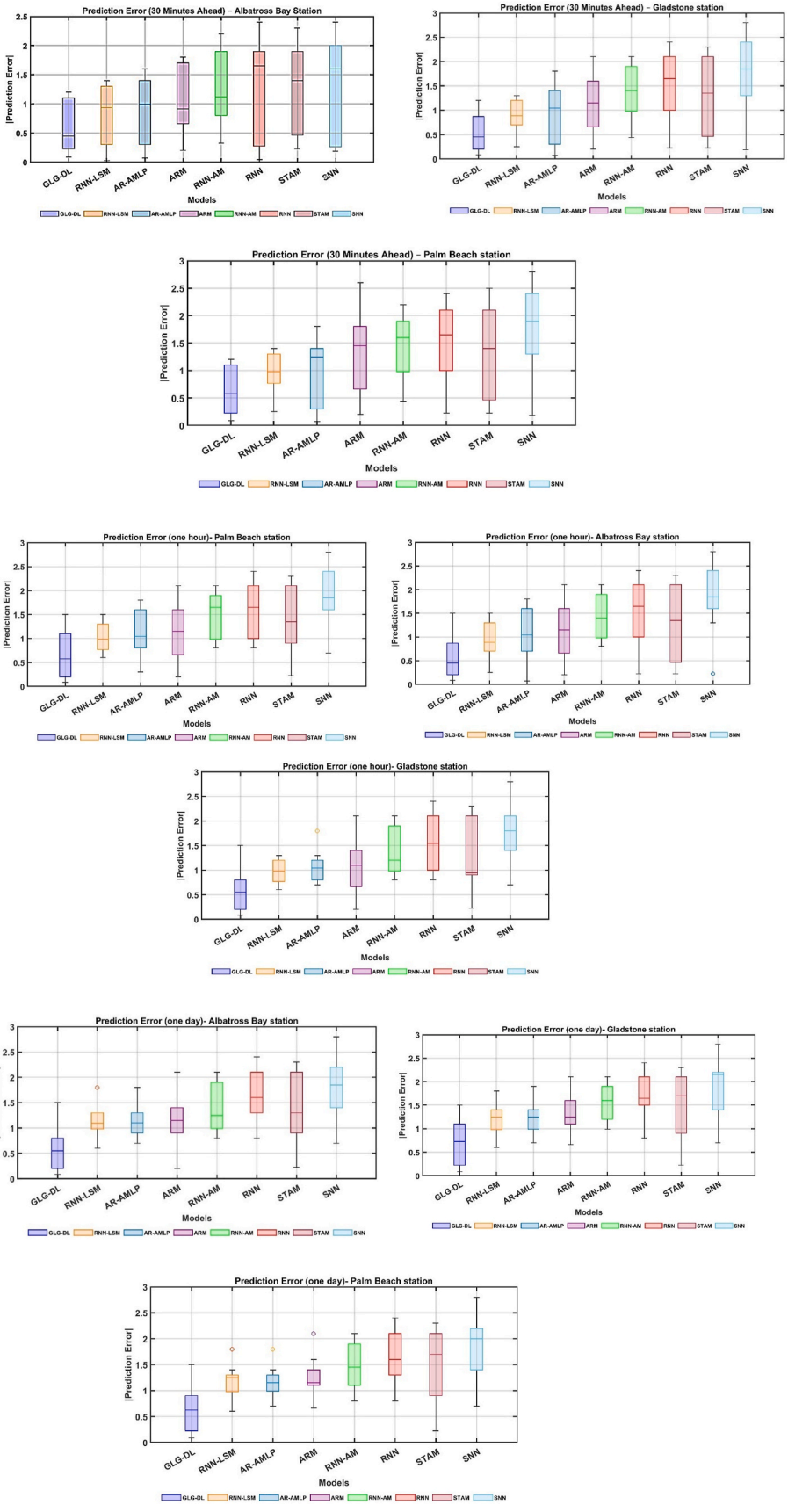

Fig. 8. 30-minutes, 1-h and one day ahead absolute prediction error |FE| of models in each station.

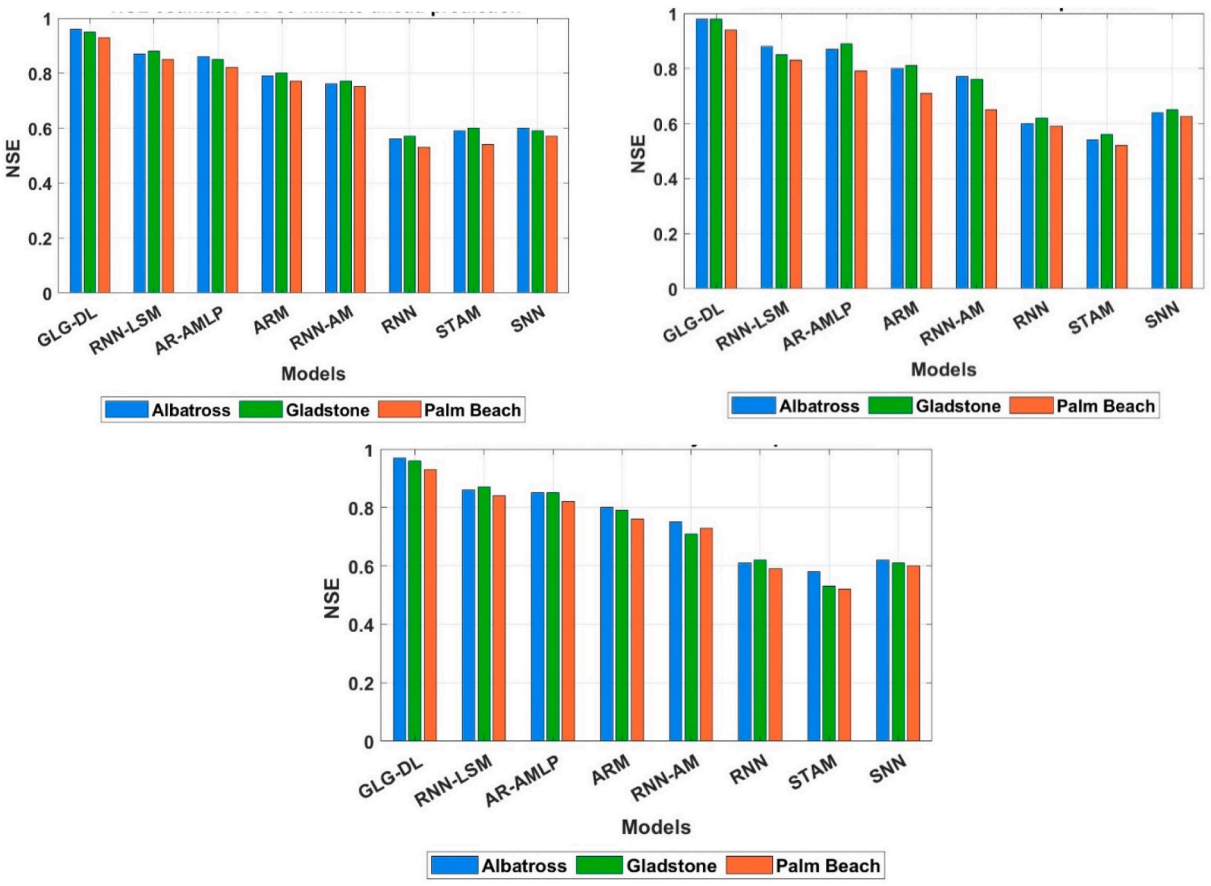

Fig. 9. Performance evaluation of each model using Nash-Sutcliffe efficiency (NSE) for 30 min, 1 h and one day ahead SWH forecasting.

recurrent gate unit (RGU) to predict multistep ahead SWH in Albatross Bay, Palm Beach and Gladstone stations. For comparison, the SNN, STAM, RNN, RNN-LSTM, RNN-AM, AR-MLP, and ARM models are also utilised to predict multistep ahead SWH. The GLG-DL model attained higher performance in terms of accuracy against the benchmark comparing models for all Albatross Bay, Palm Beach and Gladstone stations to predict multistep ahead SWH. The key findings of this research work are described as following.

- The simulation results showed that combining the global and local graph characteristics of ocean data provided a higher prediction accuracy \sed GLG-DL model allows to understand the relationships among different variables of time series data through the topology structure of graph features. The obtained results showed that the graph-based dep learning model outperforms classic deep learning approaches such as LSTM.
- The proposed model GLG-DL achieves the best results MwH. According to Fig. 4, the prediction accuracy varies with the variables used as inputs for the proposed model. In addition, experiments demonstrated that the proposed model GLG-DL performance did not show a high fluctuation over the three stations with MwH. The performance of GLG-DL was consistent with the three stations while it showed some fluctuation with other variables such as ZCW, DRiC, SST and PEW.
- The complexity of the proposed GLG-DL model was assessed in terms of complexity time as shown in Fig. 13. The floating-point operation (FLOP) was selected as an indicator to measure the complexity of the system. From the obtain results, it was evidenced that the GLG-DL model scored high FLOP counts than other models due to graph learning process consumed more time in feature analysis and extraction, while the RNN scored the lower FLOP counts compared to other models. In addition, we tested the prediction models in terms of memory usage. Based on the results in Fig. 13 it was observed that the proposed PDGDL recorded the highest memory usage as it involved several computations and matrixes for features extraction and fusing. However, The RNN, ARM and STAM models utilised less memory usage (3.86 GB, 3.8 GB, 4.0 GB respectively) as they were not hybridised with other models. Based on our observation, it was found that the complexity of models would increase when number of the employed parameters were increased. However, even though the proposed model required more computational resources, it obtained significantly higher predictive accuracy compared with the benchmark models. In future work, we will reduce the time complexity of the proposed model through applying parallelised strategies without compromising predictive accuracy.
- To shed more lights on the performance evaluation of the proposed GLG-DL model against the benchmark models, we expanded our experiment by including intermediate predictions including forecasting 3h, 6h, and 12h ahead SWH. Table 7 reports the prediction results of all models. In this experiment, the performance of the proposed GLG-DL model was evaluated in terms of RMSE, MSE, CC, and WIA against the benchmark models. The proposed model showed outstanding predictive stability across all three multistep predictions. For 3h prediction ahead of SWH, our findings showed that the proposed GLG-DL model retained accurate prediction results across the three stations Palm Beach, Albatross Bay, Gladstone, demonstrating its robust generalisability. With 6h prediction ahead of SWH, the proposed GLG-DL model demonstrated strong stability, and showed low fluctuations in RMSE, MSE. However, the RNN recorded the lowest prediction rate cross three station for 3h, and 6h prediction ahead of SWH. Table 7 also lists the results of 12h prediction ahead. It can observe that the proposed GLG-DL model

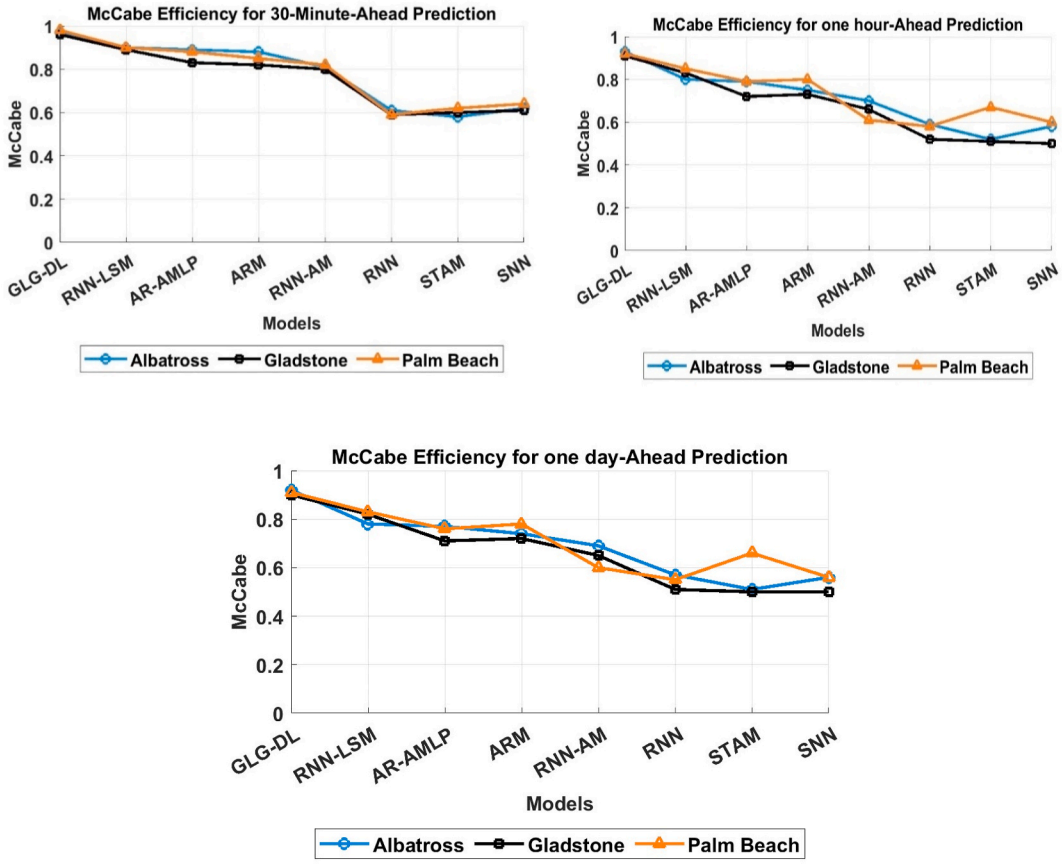

Fig. 10. Legates and MacCabe's (LM) agreement of the models in each station for 30 min, 1 h and one day ahead SWH forecasting.

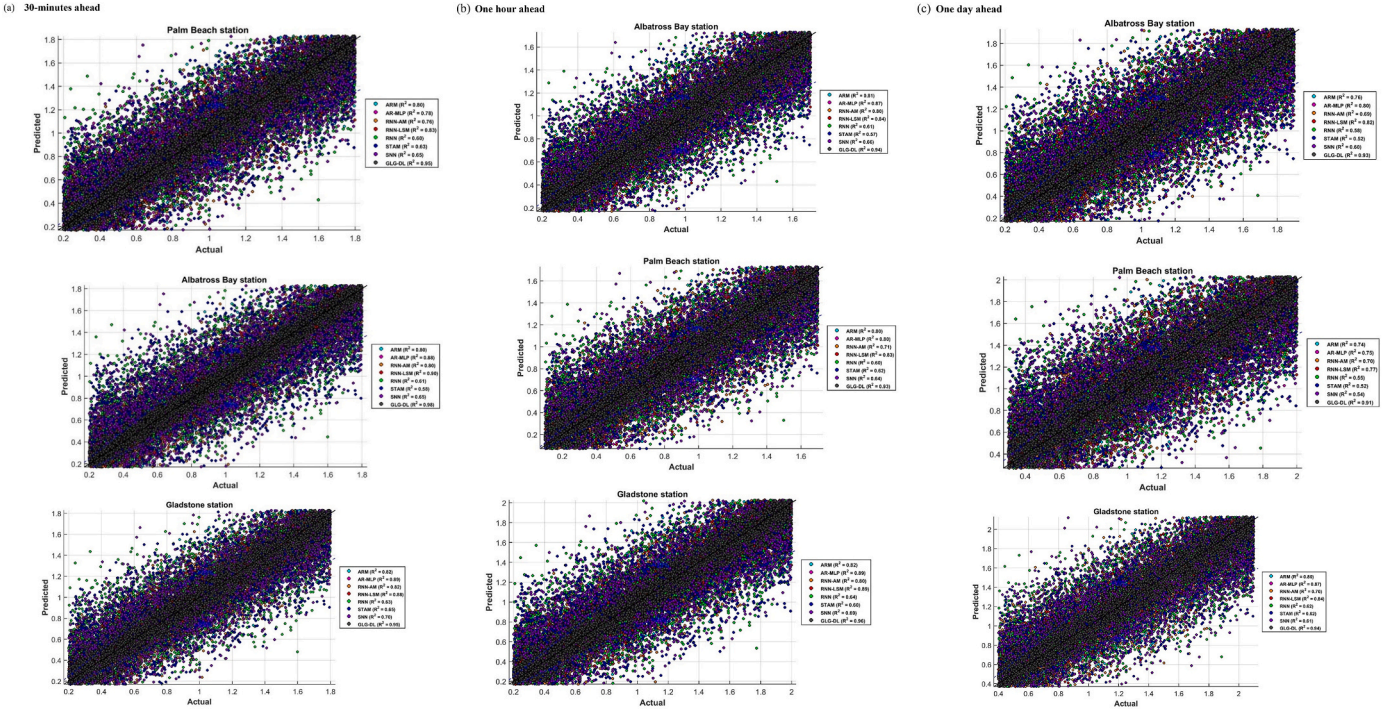

Fig. 11. Regression plots to predict (a) 30 min, (b) 1 h and (c) one day ahead SWH prediction for Albatross Bay, Gladstone, and Palm Beach stations.

attained the highest CC, and WIA values compared to the ARM, AR-MLP, RNN-AM, RNN-LSM, RNN, STAM, and SNN. Another observation, it was noticed that the AR-MLP scored the second highest CC, and WIA, and lowest RMSE, MSE cross the three stations Beach, Albatross Bay, Gladstone respectively. The obtained results in Tables 5 and 6 support our findings in Table 7, and proved that the

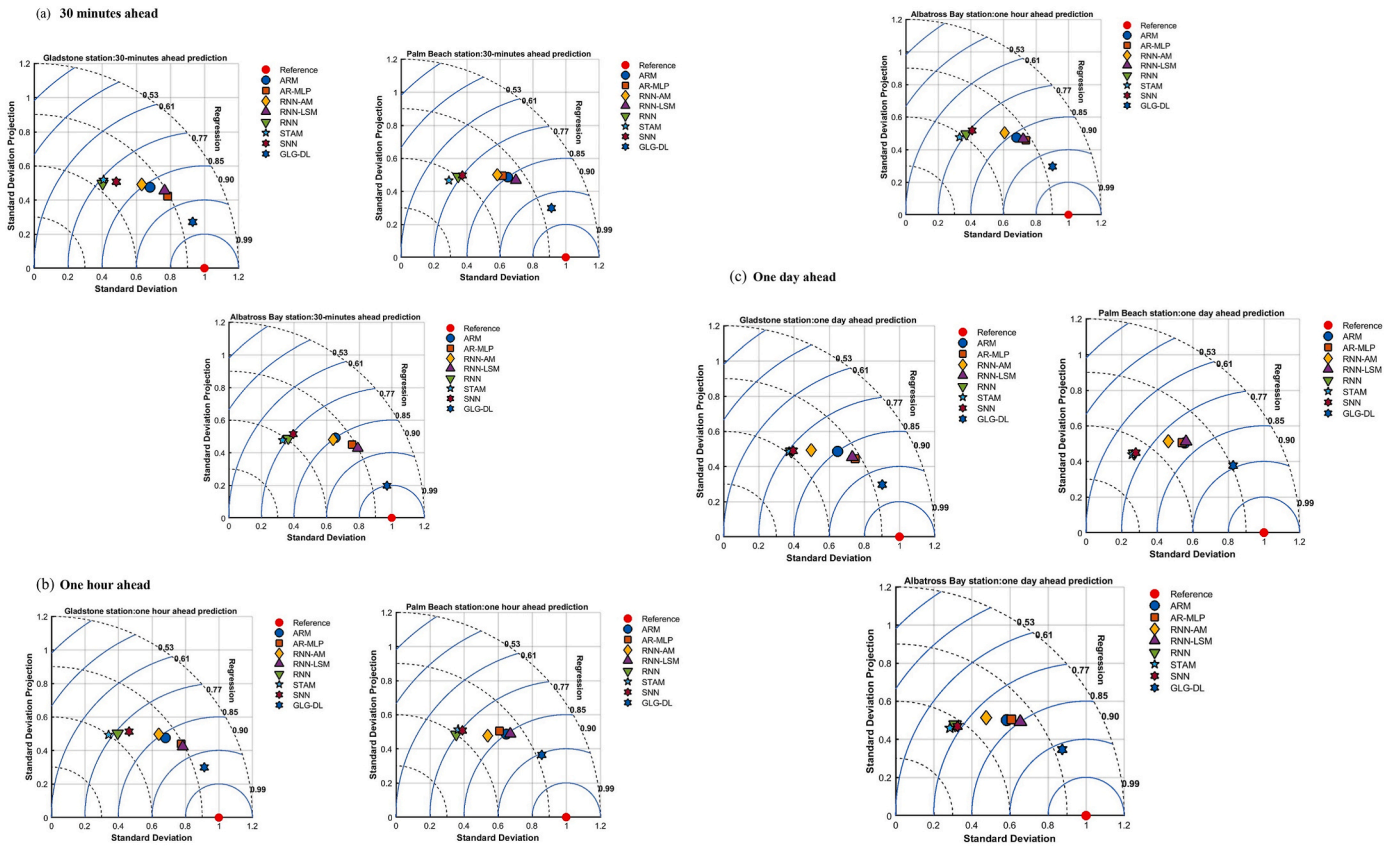

Fig. 12. Taylor diagram of GLG-DL, SNN, STAM, RNN, RNN-LSTM, RNN-AM, AR-MLP, and ARM models to predict (a) 30 min, (b) 1 h and (c) one day ahead SWH prediction.

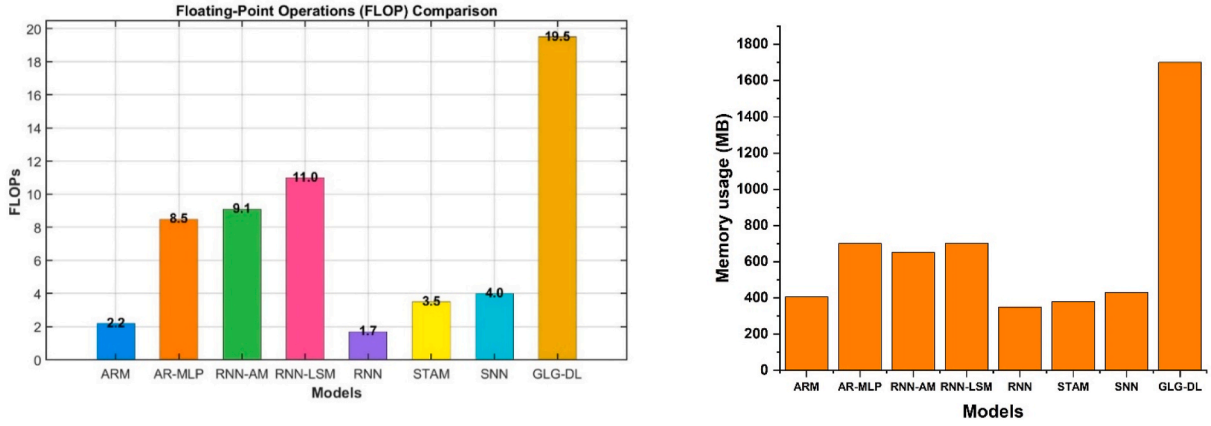

Fig. 13. Comparisons in term of model complexity using FLOP.

proposed model was an effective approach in terms of improving long-term, and short term SWH prediction.

- On of the limitations of the current study is that the proposed model was tested using data from only three sites located in Australia: Albatross Bay, Palm Beach, and Gladstone stations. While these stations provide varied coastal conditions, the geographical range remains regionally constrained. The limited geographical coverage could affect the generalisability of the proposed model, therefore, additional validation using datasets from other regions in Australia is important to fully evaluate the robustness of the proposed model in a generalized context. Another limitation of the study is that a limited set of oceanographic variables were used in this paper. Incorporating additional influential factors such as wave direction spectrum, wind speed, and atmospheric pressure can be included to further improve the predictive accuracy of the proposed model. In addition, dynamic graph architecture-based construction learning will also be adopted to fully capture the complex and dynamic relationships among variables to better understand the nature of SWH and its relationships with oceanic variables.
- The proposed GLG-DL model shows better prediction capability, but further recommendations and suggestions can be considered in the future. A possible integration of the proposed GLG-DL model with signal decomposition methods such as multivariate variational mode decomposition (ur Rehman and Aftab, 2019) and multivariate empirical mode decomposition (Rehman and Mandic, 2010) to handle the non-stationarity and non-linearity issues. Another

Table 7
SWH prediction results for 3h, 6h, and 12h ahead, the proposed **GLG-DL** against comparing models for Albatross Bay, Palm Beach, and Gladstone stations.

	Albatross Bay station											
	Prediction 3h ahead SWH				Prediction 6h ahead SWH				Prediction 12h ahead SWH			
Model	RMSE	MAE	WIA	CC	RMSE	MAE	WIA	CC	RMSE	MAE	WIA	CC
ARM	3.188	5.38	0.801	0.812	3.189	5.39	0.799	0.809	3.192	5.41	0.789	0.778
AR-MLP	2.996	3.96	0.881	0.879	2.998	3.97	0.879	0.869	2.999	3.99	0.868	0.860
RNN-AM	3.949	3.95	0.792	0.799	3.957	3.96	0.788	0.788	3.989	3.99	0.778	0.781
RNN-LSM	2.103	4.13	0.895	0.893	2.107	4.16	0.889	0.889	2.118	4.18	0.879	0.881
RNN	5.966	6.96	0.625	0.608	5.967	6.97	0.618	0.597	5.977	6.99	0.602	0.590
STAM	5.346	7.91	0.595	0.578	5.347	7.95	0.588	0.569	5.357	7.99	0.577	0.560
SNN	6.217	6.97	0.645	0.648	6.219	6.99	0.638	0.639	6.221	7.11	0.627	0.632
GLG-DL	**2.036**	**3.75**	**0.951**	**0.951**	**2.037**	**3.77**	**0.949**	**0.948**	**2.041**	**3.79**	**0.940**	**0.941**
Model	Palm Beach station											
	Prediction 3h ahead SWH				Prediction 6h ahead SWH				Prediction 12h ahead SWH			
	RMSE	MAE	WIA	CC	RMSE	MAE	WIA	CC	RMSE	MAE	WIA	CC
ARM	3.206	5.291	0.899	0.809	3.217	5.310	0.891	0.802	3.221	5.420	0.881	0.799
AR-MLP	3.733	5.481	0.779	0.789	3.742	5.490	0.770	0.781	3.752	5.520	0.769	0.778
RNN-AM	4.023	5.970	0.709	0.767	4.057	5.990	0.700	0.763	4.063	6.120	0.699	0.759
RNN-LSM	2.213	4.130	0.838	0.836	2.245	4.190	0.835	0.833	2.252	4.270	0.821	0.829
RNN	5.314	6.780	0.588	0.598	5.356	6.810	0.582	0.591	5.356	6.940	0.574	0.579
STAM	6.251	6.560	0.656	0.628	6.263	6.590	0.651	0.622	6.272	6.620	0.644	0.619
SNN	6.293	7.110	0.638	0.648	6.299	7.400	0.633	0.641	6.321	7.490	0.629	0.639
GLG-DL	**2.799**	**3.780**	**0.938**	**0.948**	**2.811**	**3.790**	**0.934**	**0.940**	**2.833**	**3.80**	**0.927**	**0.939**
Model	Gladstone station											
	Prediction 3h ahead SWH				Prediction 6h ahead SWH				Prediction 12h ahead SWH			
	RMSE	MAE	WIA	CC	RMSE	MAE	WIA	CC	RMSE	MAE	WIA	CC
ARM	3.766	5.61	0.809	0.829	3.768	5.65	0.803	0.823	3.772	5.77	0.799	0.818
AR-MLP	2.311	4.13	0.879	0.883	2.317	4.16	0.872	0.881	2.323	4.23	0.866	0.876
RNN-AM	3.121	4.13	0.768	0.793	3.126	4.17	0.761	0.791	3.131	4.34	0.754	0.787
RNN-LSM	2.812	4.37	0.888	0.886	2.818	4.38	0.884	0.880	2.823	4.45	0.875	0.877
RNN	4.945	6.23	0.638	0.634	4.948	6.28	0.633	0.630	4.954	6.36	0.628	0.625
STAM	4.994	6.91	0.577	0.656	4.997	6.96	0.572	0.651	5.11	7.00	0.565	0.647
SNN	5.322	5.99	0.687	0.697	5.327	6.11	0.681	0.692	5.345	6.28	0.678	0.688
GLG-DL	**2.021**	**3.11**	**0.976**	**0.957**	**2.025**	**3.16**	**0.973**	**0.951**	**2.035**	**3.23**	**0.967**	**0.948**

direction of the future research can be the hybridization of the explainable AI models (i.e., Local Interpretable Model-Agnostic Explanations (LIME)) (Mishra et al., 2017) and Shapley Additive explanations (SHAP) (García and Aznarte, 2020) to provide model's prediction explainability and interpretability. Additionally, physics-based models can also be incorporated with GLD-DL to illustrate the physical aspects. To understand the underlying uncertainty of the model, the Bayesian Model Averaging (Fragoso et al., 2018) and bootstrapping/ensemble (Hassan et al., 2013) strategies can be adopted. The scope of the current research can be spread in other areas of interest such as hydrology, climate change, and agricultural sectors.

7. Conclusion

In this paper, a novel graph based deep learning (GLG-DL) model has been proposed and successfully applied to predict multistep ahead significant wave hight (SWH) for three coastal regions Albatross Bay, Palm Beach and Gladstone of Queensland State, Australia. The modelling framework of the proposed GLG-DL model combines the local and global graph features to capture the main characteristics of oceanic data. The RGU was used to fuse the graph features for encoding and decoding to predict SWH. Experiment showed that the prediction accuracy of the proposed GLG-DL model was superior to the comparing models by means of numerous goodness-of-fit metrics and diagnostic plots. The proposed GLG-DL model permits to comprehend the relationships among different variables and features through the topological structure of the graph. The outcomes are expected to advance the understanding of the relationship among oceanic drivers. The research work could potentially empower the construction of a more precise and established prediction model for renewable and sustainable wave energy. The scope can be further expanded to other real applications such as climate change adaptation, water, and agriculture research areas for better understanding.

CRediT authorship contribution statement

Mohammed Diykh: Writing – original draft, Visualization, Validation, Software, Methodology, Investigation, Formal analysis, Conceptualization. **Mumtaz Ali:** Writing – review & editing, Writing – original draft, Supervision, Resources, Methodology, Investigation, Data curation, Conceptualization. **Mehdi Jamei:** Writing – review & editing, Visualization, Investigation, Conceptualization. **Ramendra Prasad:** Writing – review & editing, Writing – original draft, Conceptualization. **Abdulhaleem H. Labban:** Writing – review & editing, Supervision, Investigation, Conceptualization. **Shahab Abdulla:** Writing – review & editing, Methodology, Conceptualization. **Niharika Singh:** Writing – review & editing, Writing – original draft, Conceptualization. **Aitazaz Ahsan Farooque:** Writing – review & editing, Writing – original draft, Supervision, Investigation, Conceptualization.

Declaration of competing interest

The authors declare that they have no known competing financial interests or personal relationships that could have appeared to influence the work reported in this paper.

Acknowledgements

This Project was funded by the Deanship of Scientific Research (DSR)

at King Abdulaziz University, Jeddah, under grant no. (GPIP: 749-155-2024). The authors, therefore, acknowledge with thanks DSR for technical and financial support. The authors are thankful to the Environment and Science, Queensland Government, Coastal Data System, Queensland, Australia for providing the relevant datasets.

Data availability

Data can be available upon request.

References

Abdulla, S., Diykh, M., Siuly, S., Ali, M., 2023. An intelligent model involving multi-channels spectrum patterns based features for automatic sleep stage classification. Int. J. Med. Inf. 171, 105001.
Ali, M., Prasad, R., 2019. Significant wave height forecasting via an extreme learning machine model integrated with improved complete ensemble empirical mode decomposition. Renew. Sustain. Energy Rev. 104, 281–295.
Ali, M., Prasad, R., Xiang, Y., Deo, R.C., 2020. Near real-time significant wave height forecasting with hybridized multiple linear regression algorithms. Renew. Sustain. Energy Rev. 132, 110003.
Altunkaynak, A., Çelik, A., Mandev, M.B., 2023. Hourly significant wave height prediction via singular spectrum analysis and wavelet transform based models. Ocean Eng. 281, 114771.
Altunkaynak, A., Çelik, A., Mandev, M.B., 2024. Dynamic adaptive wavelet based fuzzy framework for extended significant wave height forecasting. Ocean Eng. 295, 116814.
Burramukku, B., 2020. Estimator Model for Prediction of Power Output of Wave Farms Using Machine Learning Methods arXiv.
Che, J., Wang, J., 2010. Short-term electricity prices forecasting based on support vector regression and auto-regressive integrated moving average modeling. Energy Convers. Manag. 51 (10), 1911–1917.
Chen, J., Li, S., Zhu, J., Liu, M., Li, R., Cui, X., Li, L., 2025. Significant wave height prediction based on variational mode decomposition and dual network model. Ocean Eng. 323, 120533.
Commonwealth of Australia, 2023. Offshore infrastructure regulator: regulating offshore renewables. from. https://oir.gov.au/guidance-and-regulation/legislative-framework#:~:text=The%20Offshore%20Electricity%20Infrastructure%20Act,and%20offshore%20electricity%20infrastructure%20projects.
Cornejo-Bueno, L., Nieto-Borge, J.C., García-Díaz, P., Rodríguez, G., Salcedo-Sanz, S., 2016. Significant wave height and energy flux prediction for marine energy applications: a grouping genetic algorithm – Extreme Learning Machine approach. Renew. Energy 97, 380–389.
Domala, V., Kim, T.W., 2023. Application of empirical mode decomposition and Hodrick Prescot filter for the prediction single step and multistep significant wave height with LSTM. Ocean Eng. 285, 115229.
Fragoso, T.M., Bertoli, W., Louzada, F., 2018. Bayesian model averaging: a systematic review and conceptual classification. Int. Stat. Rev. 86 (1), 1–28.
García, M.V., Aznarte, J.L., 2020. Shapley additive explanations for NO2 forecasting. Ecol. Inform. 56, 101039.
Gopinath, D.I., Dwarakish, G.S., 2015. Wave prediction using neural networks at new mangalore port along West Coast of India. Aquatic Procedia 4, 143–150.
Gorrell, L., Raubenheimer, B., Elgar, S., Guza, R.T., 2011. SWAN predictions of waves observed in shallow water onshore of complex bathymetry. Coast. Eng. 58 (6), 510–516.
Guo, S., Lin, Y., Feng, N., Song, C., Wan, H., 2019. Attention based spatial-temporal graph convolutional networks for traffic flow forecasting. Proceedings of the AAAI Conference on Artificial Intelligence.
Guo, Y., Si, J., Wang, Y., Hanif, F., Li, S., Wu, M., Xu, M., Mi, J., 2025. Ensemble-Empirical-Mode-Decomposition (EEMD) on SWH prediction: the effect of decomposed IMFs, continuous prediction duration, and data-driven models. Ocean Eng. 324, 120755.
Hassan, A., Abbasi, A., Zeng, D., 2013. Twitter sentiment analysis: a bootstrap ensemble framework. In: 2013 International Conference on Social Computing. IEEE.
Huang, Y., Weng, Y., Yu, S., Chen, X., 2019. Diffusion convolutional recurrent neural network with rank influence learning for traffic forecasting. In: 2019 18th IEEE International Conference on Trust, Security and Privacy in Computing and communications/13th IEEE International Conference on Big Data Science and Engineering (TrustCom/BigDataSE). IEEE.
Ibarra-Berastegi, G., Jon Sáenz, G.E., Ezcurra, A., Ulazia, A., Rojo, N., Gallastegui, G., 2016. Wave energy forecasting at three coastal buoys in the Bay of Biscay. IEEE J. Ocean. Eng. 41 (4).
IRENA, 2022. Grid Codes for Renewable Powered Systems. International Renewable Energy Agency Abu Dhabi.
Kumar, N.K., Savitha, R., Al Mamun, A., 2018. Ocean wave height prediction using ensemble of Extreme Learning Machine. Neurocomputing 277, 12–20.
Lafta, R., Zhang, J., Tao, X., Li, Y., Diykh, M., Lin, J.C.W., 2018. A structural graph-coupled advanced machine learning ensemble model for disease risk prediction in a telehealthcare environment. Big Data in Engineering Applications, pp. 363–384.
Li, Y., Yu, R., Shahabi, C., Liu, Y., 2017. Diffusion convolutional recurrent neural network: data-driven traffic forecasting. arXiv preprint arXiv:1707.01926.
Liang, Y., Ke, S., Zhang, J., Yi, X., Zheng, Y., 2018. Geoman: Multi-Level Attention Networks for geo-sensory Time Series Prediction. IJCAI.
Mahjoobi, J., Adeli Mosabbeb, E., 2009. Prediction of significant wave height using regressive support vector machines. Ocean Eng. 36 (5), 339–347.
Mahjoobi, J., Etemad-Shahidi, A., 2008. An alternative approach for the prediction of significant wave heights based on classification and regression trees. Appl. Ocean Res. 30 (3), 172–177.
Makarynskyy, O., Pires-Silva, A.A., Makarynska, D., Ventura-Soares, C., 2002. Artificial neural networks in the forecasting of wave parameters. In: 7th International Workshop on Wave Hindcasting and Forecasting. Banff, Alberta, Canada.
Malekmohamadi, I., Bazargan-Lari, M.R., Kerachian, R., Nikoo, M.R., Fallahnia, M., 2011. Evaluating the efficacy of SVMs, BNs, ANNs and ANFIS in wave height prediction. Ocean Eng. 38 (2–3), 487–497.
Mérigaud, A., Ramos, V., Paparella, F., Ringwood, J.V., 2017. Ocean forecasting for wave energy production. J. Mar. Res. 75, 459–505.
Mishra, S., Sturm, B.L., Dixon, S., 2017. Local interpretable model-agnostic explanations for music content analysis. ISMIR.
Niepert, M., Ahmed, M., Kutzkov, K., 2016. Learning convolutional neural networks for graphs. International Conference on Machine Learning. PMLR.
OES, 2023. Wave Energy Developments, Highlights, Ocean Energy Systems (OES), Aka the Technology Collaboration Programme (TCP) on Ocean Energy Systems. created by the International Energy Agency (IEA).
Özger, M., 2010. Significant wave height forecasting using wavelet fuzzy logic approach. Ocean Eng. 37 (16), 1443–1451.
Park, J., Park, C., Choi, J., Park, S., 2022. DeepGate: Global-local decomposition for multivariate time series modeling. Inf. Sci. 590, 158–178.
Rathore, N., Rathore, P., Basak, A., Nistala, S.H., Runkana, V., 2021. Multi scale graph wavenet for wind speed forecasting. In: 2021 IEEE International Conference on Big Data (Big Data). IEEE.
Raza Ul Mustafa, M., Ahmad, S.Z.A.S., Husain, M.K.A., Zaki, N.I.M., Mohd, M.H., Najafian, G., Bin Othman, I., Latheef, M., Bayu Endrayana, D., Zulaikha Bt Yusof, N., 2018. Comparison of various spectral models for the prediction of the 100-Year design wave height. In: MATEC Web of Conferences, 203, 01020.
Rehman, N., Mandic, D.P., 2010. Multivariate empirical mode decomposition. Proc. R. Soc. A 466 (2117), 1291–1302.
Reikard, G., Robertson, B., Buckham, B., Bidlot, J.-R., Hiles, C., 2015. Simulating and forecasting ocean wave energy in Western Canada. Ocean Eng. 103, 223–236.
REN21, 2023. Renewables 2023 Global Status Report Collection, Global Overview. REN21 Secretariat, Paris.
Sen, R., Yu, H.-F., Dhillon, I.S., 2019. Think globally, act locally: a deep neural network approach to high-dimensional time series forecasting. Adv. Neural Inf. Process. Syst. 32.
Shih, S.-Y., Sun, F.-K., Lee, H.-y., 2019. Temporal pattern attention for multivariate time series forecasting. Mach. Learn. 108, 1421–1441.
Smith, C., Jin, Y., 2014. Evolutionary multi-objective generation of recurrent neural network ensembles for time series prediction. Neurocomputing 143, 302–311.
Sun, L., Liu, T., Wang, D., Huang, C., Xie, Y., 2022. Deep learning method based on graph neural network for performance prediction of supercritical CO2 power systems. Appl. Energy 324, 119739.
Tao, M., Gao, S., Mao, D., Huang, H., 2022. Knowledge graph and deep learning combined with a stock price prediction network focusing on related stocks and mutation points. J. King Saud Univer.-Comput. Inform. Sci. 34 (7), 4322–4334.
ur Rehman, N., Aftab, H., 2019. Multivariate variational mode decomposition. IEEE Trans. Signal Process. 67 (23), 6039–6052.
Wang, J., Bethel, B.J., Xie, W., Dong, C., 2024. A hybrid model for significant wave height prediction based on an improved empirical wavelet transform decomposition and long-short term memory network. Ocean Model., 102367
Yu, H.-F., Rao, N., Dhillon, I.S., 2016. Temporal regularized matrix factorization for high-dimensional time series prediction. Adv. Neural Inf. Process. Syst. 29.
Yu, B., Yin, H., Zhu, Z., 2017. Spatio-temporal graph convolutional networks: a deep learning framework for traffic forecasting. arXiv preprint arXiv:1709.04875.
Zhang, Z., Li, M., Lin, X., Wang, Y., He, F., 2019. Multistep speed prediction on traffic networks: a deep learning approach considering spatio-temporal dependencies. Transport. Res. C Emerg. Technol. 105, 297–322.
Zhang, X., Zhong, C., Zhang, J., Wang, T., Ng, W.W., 2023. Robust recurrent neural networks for time series forecasting. Neurocomputing 526, 143–157.
Zhao, J., Deng, F., Cai, Y., Chen, J., 2019. Long short-term memory-fully connected (LSTM-FC) neural network for PM2. 5 concentration prediction. Chemosphere 220, 486–492.
Zhao, S., Lin, S., Li, Y., Xu, J., Wang, Y., 2020. Urban traffic flow forecasting based on memory time-series network. In: 2020 IEEE 23rd International Conference on Intelligent Transportation Systems (ITSC). IEEE.
Zhao, L., Li, Z., Pei, Y., Qu, L., 2024. Disentangled Seasonal-Trend representation of improved CEEMD-GRU joint model with entropy-driven reconstruction to forecast significant wave height. Renew. Energy 226, 120345.
Zheng, Z., Ali, M., Jamei, M., Xiang, Y., Abdulla, S., Yaseen, Z.M., Farooque, A.A., 2023. Multivariate data decomposition based deep learning approach to forecast one-day ahead significant wave height for ocean energy generation. Renew. Sustain. Energy Rev. 185, 113645.